PREDICTION OF "FIRST DOSE IN HUMAN" FOR RADIOPHARMACEUTICALS / IMAGING AGENTS BASED ON ALLOMETRIC SCALING OF PHARMACOKINETICS IN PRE-CLINICAL ANIMAL MODELS

by

David Charles Onthank

A Dissertation

Submitted to the Faculty of the

WORCESTER POLYTECHNIC INSTITUTE

In partial fulfillment of the requirements for the

Degree of Doctor of Philosophy

in

Biomedical Science

December 2005

APPROVED:

Dr. Joseph C. Bagshaw, Major Advisor, Worcester Polytechnic Institute

_____

Dr. Helen G. Vassallo, Committee Member, Worcester Polytechnic Institute

_____

Dr. Simon P. Robinson, Committee Member, Bristol-Myers Squibb Medical Imaging

_____

Dr. Robert W. Siegler, Committee Member, Bristol-Myers Squibb Medical Imaging

_____

ABSTRACT

It is an FDA requirement that the "first in human" dose be based on pre-clinical animal model efficacy and safety testing to ensure a safe entry into Phase I clinical trials. Pre-clinical safety and efficacy models range from mouse to non-human primates. Interspecies scaling of pharmacokinetic parameters is therefore important for predicting drug doses in human clinical trials, although it continues to be less than optimal. Understanding the disposition of the compound in different species through *in vitro* and *in vivo* experiments is necessary to ensure appropriate species are selected for human estimates. Data for three imaging agents and a pharmacological stress agent (Oncology tumor agent (DPC-A80351), Thrombus agent (DMP-444), Infection agent (RP-517) Pharmacological stress agent (DPC-A78445-00)) that entered clinical trials and an imaging agent being developed (RP845), were assessed for scaling accuracy. Initially, pharmacokinetic data from animal models were used to extrapolate to human though body weight allometric scaling. Subsequently, the impact of adjusting for plasma protein binding and the impact of metabolic stability in the different models were examined.

Allometric scaling of animal pharmacokinetic parameters (clearance (CL), half-life (t½) and volume of distribution (Vd_{SS})) achieved a prediction of the human pharmacokinetic parameter within 13 to 109% of the observed values. This prediction was further improved by adjusting for plasma protein binding of the drug, and achieved an estimate within 5 to 57% of the clinically observed values. Since the parent compound

was the dominant species (>95%) in the circulation, metabolic stability was not used as a correction factor.

Weight based allometric scaling was further examined for an atherosclerotic plaque targeted radiopharmaceutical imaging agent, RP845-Tc-99m, currently in development. Pharmacokinetic parameters were determined in mouse, rat and rabbit followed by allometric scaling to predict the non-human primate values. Differences between predicted versus observed non-human primate Cl, t½ and Vd_{SS} were 40%, 52% and 8%, respectively. Correcting for plasma protein binding improved the prediction for Cl and t½ to within 12 and 3 %, respectively. The Vd_{SS} prediction, however became less accurate (38% difference). Since blood clearance is the major parameter in predicting human dose, the improvement from 40% to 12% was important. The plasma protein binding adjusted animal data was then used with allometric scaling to predict human CL, t½ and Vd_{SS}. The predicted values were 7.6 mL/min/kg, 70.6 minutes and 0.87 L/kg respectively. Based on the predicted human blood clearance and the dose required to image atherosclerosis in a rabbit model, the estimated human dose would be unacceptably high. This demonstrates how allometric scaling can be used in research projects to assess clinical feasibility.

The impact of metabolism differences influencing the reliability of various species to predict for man was highlighted by DPC-A78445-00. DPC-A78445-00 is being developed as an alternative to exercise in myocardial perfusion imaging for the evaluation of coronary artery disease. DPC-A78445-00 was rapidly metabolized to the

carboxylic acid by mouse and rat blood *in vitro* and *in vivo*, however longer stability was observed in the dog. *In vitro* human blood data was consistent with the dog, suggesting that mouse and rat would not be representative species. DPC-A78445-00 plasma protein binding was at a similar, moderate level in rat, dog and human plasma and metabolism by hepatocytes was similar in dog and human. Phase I human clinical trial testing determined the area under the blood concentration-time curve (AUC) and clearance predicted by the dog were within 32% of the human values.

Overall, body weight based allometric scaling of pharmacokinetic parameters from animal models, when corrected for plasma protein binding, yielded reliable predictions of the human pharmacokinetics (within 50%) for radiopharmaceutical imaging agent. However, although predictive scaling from animal data can give insight into feasibility of compounds working in human, it is important to identify species differences with respect to metabolic stability. This allometric scaling method provides an additional tool to better predict doses in human for novel Medical Imaging agents.

ACKNOWLEDGEMENTS

-This work is dedicated to my family for their loving support throughout my graduate studies-

Foremost I would like to thank my wife, Christine, for her endless support, love, and continuous encouragement throughout my graduate studies.

Thank you to my children, Dan and Kaitlin for their love and understanding over the past four years and to my parents for their support throughout my life and encouragement during my graduate education.

As I reflect on the past five years through my graduate program at WPI, I realize how I have grown both professionally and personally. I have had the opportunity to meet wonderful individuals whose scientific knowledge and friendship have been immeasurable.

I would like to thank my committee members;

- Joe Bagshaw for directing my course of study and enabling me to pursue my Ph.D. Degree through the part-time college consortium program.

- Simon Robinson for his tremendous guidance, scientific contributions and broad knowledge of the sciences whom I respect and admire.

- Helen Vassallo for providing valuable scientific suggestions and comments throughout this project.

- Bob Siegler for his wisdom and scientific contributions throughout my graduate studies.

In addition I would like to thank;

- Eric Overstrom, Biology and Biotechnology Department head, for his leadership and program guidance.

- Carol Butler for her friendship and tremendous organizational skills keeping my program on track.

- My Bristol-Myers Squibb Medical Imaging Research Biology and Chemistry colleagues whose support through their talented research skills and friendship has been immeasurable.

TABLE OF CONTENTS

PAGE

LIST OF TABLES

PAGE

LIST OF FIGURES

PAGE

1. CHAPTER I

1.1 Background and general overview

1.1.1 Overview statement

Predicting the pharmacokinetics of radiopharmaceutical imaging agents in humans from pre-clinical animal models with high accuracy would result in a safer more efficacious selection of first dose in clinical trials. Fewer dose ranging studies, subjects, and clinical trials would be necessary and could result in a shorter time for introducing a drug that meets an unmet medical need. Translating how the body distributes and clears the drug in animals into a best estimate of the human condition is difficult. For therapeutic agents, dose prediction has been attempted with various scaling methods and a wide range/number of animal models, various drug characteristics/dispositions and different routes of drug administration. The predicted effective dose for new imaging agents entering Phase I studies at Bristol-Myers Squibb Medical Imaging (BMS-MI) has often been based on the non-human primate or a species seen to be representative of the human based on *in vitro* testing (i.e. hepatocyte assays). Human dose prediction from the "relevant" species has typically been based on a body weight extrapolation and has not utilized all the data available. The research project described below examines the use

of allometric scaling to better utilize the information from all the animal models to predict the safe and efficacious clinical dose for medical imaging agents.

1.1.2 Pharmacokinetics

Pharmacokinetics is the study of what the body does to a drug as opposed to pharmacodynamics, which is what the drug does to the body. To better define pharmacokinetics, the acronym "ADME" is used which stands for absorption, distribution, metabolism and excretion. Absorption is the process by which a compound and its metabolites are transferred from the site of application (intravenous (IV), intramuscular (IM), subcutaneous (SubQ), oral, inhalation, topical) to the systemic circulation. In the case of radiopharmaceutical medical imaging agents, the drug is typically administered intravenously and therefore has 100% absorption. Distribution is where the drug locates following absorption. This is determined by measuring the concentration of drug in tissues and organs either by collecting samples (biodistribution) or imaging. Metabolism is the conversion of the parent agent to metabolites. These are detected and identified by sampling tissues, plasma, urine, bile, and feces. Blood and liver (cytochrom P450) are the two main organs of the body that metabolize drugs, with other tissues in the body (kidney, lung) also capable of metabolic activity to a lesser degree. Excretion is the route and rate of elimination of the agent from the body. This is typically determined through tissue distribution and mass balance studies. The two major clearance routes for most agents are renal or hepato-biliary.

1.1.3 Pharmacokinetic parameters

Pharmacokinetic parameters that have been used for scaling from pre-clinical animal models to humans are A) blood clearance (CL), B) terminal half-life (t1/2) and C) volume of distribution at steady state (Vd_{ss}). These are defined below:

A) Blood clearance is the rate an organ system totally extracts a drug from plasma. The units for clearance are mL plasma/minute/kg body weight and is calculated as: CL = Dose/Area under the blood concentration-time activity curve (AUC).

B) The terminal half-life of a drug is the time required for the plasma concentration to decrease by 50% after absorption and distribution are complete. Terminal half-life is expressed in time (min, hr) and is calculated as: T1/2= 0.693/slope of the blood concentration-time curve.

C) Volume of distribution describes the extent of distribution of a drug and is useful in determining the size of the dose required to reach the desired blood concentration of the drug. The units are expressed in L/kg and is calculated as: Vdss = (Dose x AUMC)/ (AUCinf X AUCinf) (AUMC=area under the moment curve, AUCinf= area under the curve from time zero to infinity). Volume of distribution of the central compartment can play an important role in establishing the safety or toxicity for first dose in humans. Since the administered dose is known, the predicted Vdss can be used to calculate the plasma concentration of a drug at time zero following an intravenous injection.

These three parameters provide information for determining total exposure of a drug to the target and non-target organs with a given dose. They are therefore appropriate parameters to use when scaling the potential efficacy or toxicity from species to species

1.1.4 Radiopharmaceuticals

Radiopharmaceuticals play an integral role in clinical nuclear medicine by providing a tool to better understand human disease and develop effective treatments. Nuclear medicine continues to grow with the commercial availability of new radioisotopes and the discovery of novel radiopharmaceuticals. The properties of a radioisotope such as the half-life (decay time to reach half the starting radioactivity) and the type of radiation emitted (i.e. gamma, beta, positron) are important selection criteria for either diagnostic or therapeutic use. The path length or distance traveled by the radiation is an important consideration in selecting the isotope. For instance, in the case of a diagnostic imaging agent, high penetrating gamma rays would be preferred with isotopes such as technetium-99m, inidum-111, thallium-201, gallium-67 and iodine-123 to effectively penetrate through the body for detection with a gamma camera. In contrast, if a radiopharmaceutical is delivered in close proximity to a tumor for therapeutic applications, the isotope would have a short path length and high energy such as iodine-131, strontium-89, renium-186, yttrium-90 and phosphorus-32. The radiohalogens, for example, were responsible for some of the early growth in nuclear medicine with iodine isotopes, such as ^{131}I, ^{123}I and ^{124}I for diagnosis and therapy (ie imaging and treatment of thyroid diseases). The use of short lived single photon emitted computed tomography

(SPECT) isotopes, such as ^{201}TI, ^{111}In and ^{67}Ga, are continuing to grow for diagnostic imaging of the heart, tumors and sites of inflamation/infection.

A radiopharmaceutical is typically comprised of three components: a targeted ligand, a linker/spacer with pharmacokinetic modifying properties (PKM) and the chelator for carrying the radionuclide (Figure 1.1). Each of the components can vary in size (molecular weight) depending on the unique isotope being chelated to the molecule, the length of the spacer required for the desired pharmacokinetic profile and the targeting ligand. The ligand is designed to have high affinity for a selected receptor and is either an agonist or antagonist, which has no pharmacological effect at levels administered (Silverman, R.B., 1992). The linker portion of the molecule can act as a spacer to potentially alleviate steric hinderance of the receptor/ligand binding interaction or as a pharmacokinetic modifier, which plays a role in changing the disposition of the molecule in the body with respect to blood clearance, binding to target/background tissues and/or route of clearance (Crum-Brown and Fraser, 1868 ; Silverman, R.B., 1992).

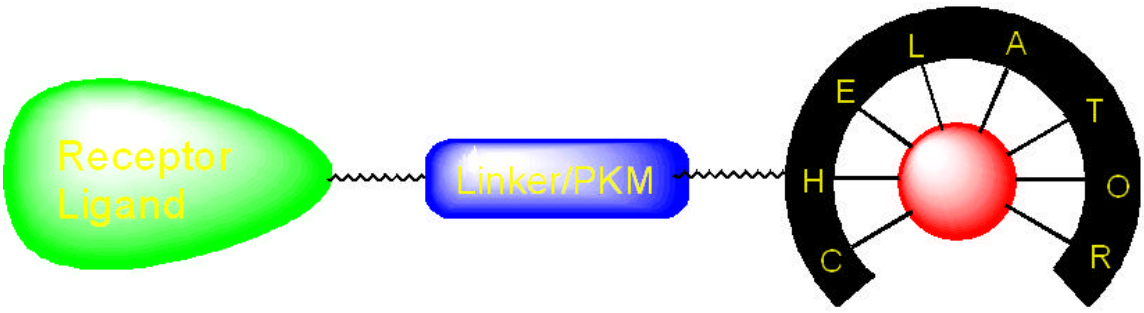

Figure 1.1 Radiopharmaceutical components

Radiopharmaceutical diagnostic imaging agents are typically dose limited by the radioactivity administered as opposed to the absolute amount of active ligand, which typically limits a therapeutic agent. This is due to the high specific activity of the radiopharmaceutical, which means that the mass of the active ligand is small relative to the radioisotope. A maximum for the radioactivity dose would be reached before observing a physiological effect from the trace amount of ligand. In most cases, an ideal radiopharmaceutical imaging agent targets with high affinity, clears the blood rapidly, has low plasma protein binding, is stable in the circulation and is excreted predominantly through the kidneys. These criteria are required to achieve the highest target to background binding of the compound to allow clear visualization of the intended target with the selected imaging modality. Radiopharmaceutical imaging agents, as opposed to therapeutic agents, vary in the required amount of active drug administered to achieve the desired result. Imaging agent drugs are administered in the μg/kg range whereas therapeutics are administered in the mg/kg range (Focan *et. al*., 2005; DeNardo *et. al.*, 2003). These low doses typically will not saturate enzyme, receptor or clearance mechanism and therefore make pharmacokinetics easier to interpret.

1.1.5 Interspecies scaling

"Overall, though interspecies scaling of pharmacokinetics requires refinement and better understanding, the approach has a lot of potential during the drug development process" (Mahmood *et al*, 1999). Mahmood, whose work at the Food and Drug

Administration (FDA) has established him as a leader in the field of interspecies scaling, captures the scientific value of utilizing scaling techniques for increased success and speed of providing drugs for unmet medical needs. Many interspecies scaling methods have been used, including: MLP (Maximum life-span potential), brain weight, BSA (Body Surface Area), physiological-based models and allometric scaling as ways to better predict the fate of drugs administered to humans using pre-clinical data. Varying degrees of success have been achieved among these techniques when applied to different drug types over the past several years. However, there still remains controversy among investigators as to the best prediction methods and the value of using body weight or body surface area. Early studies by Dreyer and Ray (1910) indicated that the ratio of blood volume to body surface area was constant in rabbits, guinea pigs and mice but decreased with increasing body weight. Baker *et al*. (1957) also reported that body surface area is predictive for total blood volume in normal adults, but not across species. These studies, as well as others, suggest that the use of body surface area to correct between different species may work well within a small size range for some parameters, however, may not be linear across the board for all species and physiological parameters. Pinkel (1958) however, was able to correlate body surface area directly to the total number of glomeruli and to the kidney weight of different mammalian species (rat, dog, and human). Overall, body surface area has proven difficult to use as a tool for pharmacokinetic predictivity.

Lombardo and colleagues in 2002 proposed the use of physiochemical parameters of the drug such as logD and pK_a values to predict volume of distribution in humans.

They reported accuracy within 2-3 fold of the observed value and concluded that the advantage of optimizing this approach would reduce the use of animals for pharmacokinetic studies.

Two approaches of interspecies scaling have been reported extensively in the literature over the past decade. These approaches include physiological based pharmacokinetic models (PBPK) and allometric methods. Both methods have advantages and disadvantages and vary significantly in their ability to predict interspecies scaling depending on the therapeutic drug, route of administration and mechanism/mode of action. PBPK models employ mechanistic based evaluation of drug disposition and are mathematically complex, time consuming models. Allometric scaling employs the hypothesis that body weight scaling of pharmacokinetic parameters is possible for predicting interspecies doses of a therapeutic drug. It is, however, currently unclear whether allometric scaling will provide a good prediction for medical imaging agents that are generally intravenously administered and often have a higher molecular weight than therapeutic agents.

1.1.6 Allometric Scaling

Allometric scaling is an interspecies scaling method that employs log transformation of body weight and pharmacokinetic parameters to extrapolate from animal models to humans.

The following equation defines allometric scaling;

$$Y = aW^b$$

Y = physiological parameter (CL, t½, Vd_{SS})

a = allometric coefficient

W = body weight

b = allometric exponent

The equation can also be expressed as:

$$Y = \log a + b \log W$$

(a = y intercept, b = slope)

Many physical and physiological parameters have been shown to correlate with body weight in animals as well as humans (Boxenbaum *et al*., 1982; Bonati *et al*., 1984; Dedrick *et al*., 1970; Mordenti, 1986). Weiss and co-workers (1977) assumed on this basis that pharmacokinetic parameters would also correlate with body weight and evaluated the extent to which clearance rates and biological half-lives are related to body weight. They used a simple allometric equation and made certain assumptions that drug metabolism occurs only in the liver and that liver clearance is contingent on hepatic blood flow. They found scaling correlates body weight to blood flow using body weight to the 0.75 power. This works in the ideal situation, however metabolism is frequently unrelated or not limited by hepatic blood flow, which adds complexity to the prediction. Weiss

concluded, “Since the exponents of the allometric equations (for blood flow, enzyme activities, and renal excretion parameters) as well as experimental values have an exponent near 0.7 (i.e. body weight to the 0.7 power), it is possible (even if the elimination mechanism is not known) to describe, in many cases, the approximate correlation’s between and within species.” Other investigators have also suggested for many years that the basal metabolic rate scales as the 2/3 or ¾ power of the body mass and may be used to predict pharmacokinetics (Schmidt, 1983; Calder, 1984; West *et al*., 1997; West *et al*., 1999; Kleiber, 1932; Heusner, 1982; Feldman *et al*., 1983; Banavar *et al*., 1999; Dodds *et al*., 2001). This example of the body weight rule (ie. rule of exponents) is a useful tool for investigators to obtain a general guideline for making reasonable interspecies predictions, however improvements to this method would be necessary to obtain qualitative, accurate extrapolations.

In addition to differential metabolism affecting interspecies variation, species differences in absorption, plasma protein binding, biliary excretion, glomerular filtration and intestinal fluora also play key roles in interspecies predictions. Recently, investigators (Nagilla *et al*., 2004) reported a method of allometric scaling using various correction factors including: brain weight, maximum life-span potential and glomerular filtration. Results of their studies indicated a predictive success rate between 18 to 53% with no increase in accuracy using the correction factors. They concluded that allometric scaling with or without their correction factors was sub-optimal in predicting human clearance based on *in vivo* pre-clinical data.

Caldwell and co-workers (2004) presented the possibility of predicting human clearance, volume of distribution and terminal half-life through allometric scaling of *in vivo* rat data alone. They concluded that dividing rat clearance, volume of distribution and terminal half-life by 40, 200 and 4, respectively, a reasonable qualitative estimate would allow for go/no-go human pharmacokinetic decisions for drug discovery candidates. This approach may be useful for preliminary estimates of toxicology doses.

1.1.7 Selection of Species

The number of species used for prediction and ensuring a range of body weights among the species tested are important factors to consider when applying allometric scaling. If body weights have less than a 5-10 fold range, the slope of the extrapolated line is not well defined and can easily skew the determined human value. Having a varied range of body weights better defines the slope for extrapolation to a 70 kg human (Figure 1.2). If a species with a body weight greater than 2-3 kg was used instead of the mouse model (0.025 kg) in this example, the body weights of the three species used for extrapolation would be close together and potentially skew the extrapolated human estimate.

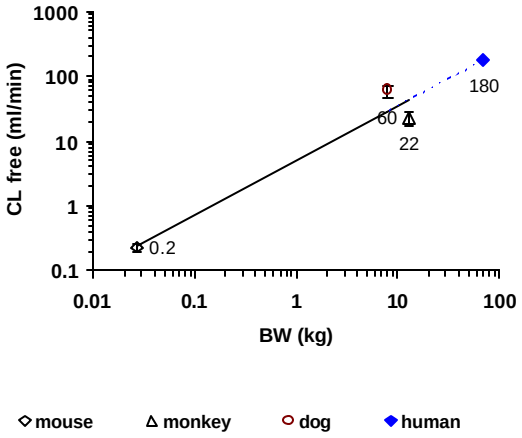

Figure 1.2 Example of blood clearance extrapolation from animal models to human.

Mahmood and co-workers (1996) investigated the efficiency of using two versus three species for prediction of clearance and volume of distribution of drugs in humans using allometric scaling. Their findings suggest that three species are needed for prediction of clearance, however volume of distribution is predicted equally well using data from two or three species. The Drugs examined in Mahmood's study had either renal or hepatobiliary clearance and varied between 15- 80% protein binding. No corrections were made to the results based on clearance route or protein binding which may explain the 1- 373 % error between observed and predicted values. Often it is presumed that the more species used in the prediction model the more reliable the result (Mahmood *et al.*, 1996). Although this may be true in some cases, each additional

species tested requires time, resources and additional animals. The degree of improvement to the final prediction would need to be evaluated.

1.1.8 Plasma Protein Binding

Plasma protein binding is the amount of drug bound to plasma proteins in the circulating blood that is typically determined through ultrafiltration centrifugation or membrane dialysis techniques. Plasma protein binding plays a critical role in determining the distribution and clearance of a drug from the blood circulation. Some drugs have limited association with the constituents of blood when administered while others associate or bind to albumin, globulins, lipoproteins and erythrocytes. Albumin (~68,000 MW) is the major drug binding protein in plasma comprising 50-60% of the total protein (Goldstein, 1949; Meyer and Guttman, 1968; Koch-Weser and Sellers, 1976). Only drugs that are unbound or free in circulation are capable of diffusing through vessel walls to reach the site of action or be excreted. The plasma protein bound drug is maintained in the circulation longer and is released as the free drug concentration decreases. Free drug is then available for metabolism, excretion or distribution outside the vasculature. Blood concentration-time plots usually show a slower clearance profile over time with increasing plasma protein binding. If a drug is highly protein bound, the intensity of its effect may be diminished, however the duration of exposure will be longer, possibly resulting in an extended effect on the target. In the majority of cases,

protein binding is a reversible process that maintains equilibrium in the blood over time (Calabrese E.J., 1946).

According to Koch-Weser and Sellers (1976), albumin carries a net negative charge at a physiological pH of 7.3, but is capable of interacting with both positive and negative charges on drugs. The different binding interactions include electrostatic, hydrogen bonds, hydrophobic bonds and dipole bonding. Typically, more highly bound drugs have a lower solubility in water and hydrophobic binding to albumin can be significant (Calabrese, E.J., 1946). This is true with increasing carbon chain lengths having an affect on higher protein binding. In general, Goldstein (1949) concluded that affinity is increased for large molecules, particularly those containing aromatic rings, which can contribute to van der Waals forces to the bond energy. Carbon chain length, amino acids, aromatic rings, radioisotope chelators and linkers are among the modifications used in imaging programs to maximize the targeting potential of the drug. An important consideration in optimizing the SAR of an imaging agent is ensuring the drug's characteristics are also optimized relative to visualization of the diagnostic target. Maintaining low protein binding, which in turn clears the drug from the general circulation and non-target background tissues faster, will help achieve this goal. In contrast, therapeutic drugs often require a long duration of action that can be achieved by increasing plasma protein binding, which in turn increases circulating half-life of the drug. Plasma protein binding plays an important role in correcting for allometric scaling predictions only if there are significant differences in the amount of drug bound between the species used for modeling. "When protein binding is low, it will not exert a major

influence on allometric scaling, however if high or varies between species, it may be appropriate to scale unbound drug" (Mordenti *et al*., 1985)

Witiak and Whitehouse (1969) generally observed that human serum albumin typically bound higher levels of drug than albumin of other species. They found that human serum bound more drug than rat serum 13 times of 22; 16 of 22 times when compared to dog serum; 10 of 16 when compared to rabbit serum and 7 of 10 when compared to mouse serum. However, in monkey serum this pattern was not observed with only 7 out of 14 times that human serum bound more drug. These differences may be explained by the varying amounts of albumin per species or simply by structural differences in the albumin from different species. Plasma protein binding is clearly a multi-faceted phenomenon that is vastly complex and requires further investigation.

1.1.9 Metabolic stability

The metabolic stability of a drug can vary among species and influence the pharmacological effects of the drug, toxicity of the drug and route/ rate of clearance from the body. Understanding the types of metabolic processes the drug undergoes *in vivo* is important when trying to interpret pharmacokinetic results. Briefly, drug metabolism is classified in two phases. Phase I are oxidation, reduction and hydrolyses reactions which can form products that proceed to Phase II reactions. Phase II reactions are conjugations (i.e. glucuronidation, glutathione addition) that ultimately make the drug metabolites

more polar expediting renal excretion and lowering the chance of toxicity. Williams (1967) points out that interspecies drug metabolism must focus on the qualitative and quantitative differences in the activity and specificity of the enzymes catalyzing both Phase I and II reactions. Interspecies differences in metabolism may result from differences in a) the absolute amount of an enzyme, b) the amount of a natural inhibitor of the enzyme, c) the activity of an enzyme reversing the reaction, and d) the extent of competing reactions using the same substrate. Drugs metabolized by both Phase I and II reactions may be excreted as 1) the original substance, 2) products of the Phase I reaction, and 3) conjugation products (Williams, 1967). The proportion of each excreted will vary significantly between species. Caution should be exercised when interpreting interspecies differences in metabolism without considering other important variables, such as: age, diet, sex, stress, route of administration, size of dose, diurnal variation, season of the year and daily temperature (Calabrese, E.J., 1946). Blood stability of a radioactive compound is typically measured after extraction of the drug from the blood following protein precipitation, by high-pressure liquid chromatography (HPLC). All radioactive entities are separated, counted and individually integrated to determine the percent of intact parent drug in the sample. The radioactive counts represent the total activity in the blood sample, however they do not provide information on the chemical nature of the species being detected. The total counts could be a mixture of intact parent drug, metabolites and unbound radioactive isotope. If the metabolic profile of the compound is unknown and the compound is not completely intact, the drug could appear to be clearing faster or slower from blood because the assay is measuring a metabolite

clearing and not the parent compound. These are important factors to consider when interpreting pharmacokinetic results.

1.1.10 Synopsis

This dissertation research has been focused on the issue of predicting pharmacokinetics from pre-clinical animal models to humans and ultimately selecting an efficacious dose for clinical trials. An efficacious dose in humans is based on achieving the same blood exposure as observed in the animal models that had effective drug accumulation at the target. Pharmacokinetic differences between species with respect to how the body handles a drug have been reviewed from the literature. There are clear differences within and between species that makes prediction of pharmacokinetics extremely difficult, although investigators have described various methods to attempt inter-species scaling. The methods currently used for prediction include physiological-based models, allometric methods and body surface area (BSA) calculations, however there is still variability and poor correlation between species depending on the drug class. Medical imaging agents are typically intravenously administered, small, hydrophilic compounds that are rapidly excreted from the body via the kidneys. These compounds are ideally not metabolized, however may have a range of serum protein binding as a percent of total circulating drug that would alter clearance from the blood and potentially limit availability to the target.

The research outlined below examines the use of the allometric method of scaling, including correction factors, between species from recent projects at BMS Medical Imaging. This has extended previous work describing the usefulness of this method for therapeutic molecules in medical imaging tracers. The ability to predict the pharmacokinetics of a drug from pre-clinical animal models for clinical trials in humans would provide a major enhancement to the compound selection and the safe progression of drugs into clinical development.

2. CHAPTER 2

2.1 Hypothesis and Objectives

2.1.1 Research Hypothesis

Efficacious and safe doses of Radiopharmaceuticals / Imaging agents in humans may be predicted from pre-clinical animal models through allometric scaling and "correction factors" associated with the pharmacokinetic fate of the drug. These correction factors may include adjusting predictive values based on extent of plasma protein binding and metabolic stability of the drug.

The goal is to produce a mathematical formula that predicts human pharmacokinetics (less than 30% difference between predicted and observed values) from administration of the radiopharmaceutical imaging agent in animal models. This model may provide a more accurate prediction of drug pharmacokinetics in humans based on interspecies scaling of pre-clinical models providing a more robust estimation of an efficacious first dose in human.

2.1.2 Experimental Objectives

The specific and technical objectives of this project are to:

- Apply allometric scaling to pre-clinical and clinical data from recent Medical Imaging programs to assess how well human pharmacokinetics was predicted.
- Adjust the allometric scaling model for differences in plasma protein binding and metabolic stability for each of the compounds. Re-evaluate the predicted versus observed results.
- Test a novel Tc-99m labeled plaque-targeting imaging compound in mouse, rat, rabbit and primate.
- Apply the allometric method of scaling with correction factors between species for the plaque targeting imaging agent and predict pharmacokinetics in primate. Evaluate prediction, then use all species to predict human pharmacokinetics.
- Evaluate an A2a coronary vasodilator in pre-clinical models through *in vitro* testing and assess the role of each model in allometric scaling

3. CHAPTER 3

Prediction of Human Pharamacokinetics for Radiopharmaceutical Imaging Agents from Animal Models using Allometric Scaling

3.1 Summary

Allometric scaling with and without correction for plasma protein binding was applied to animal model pharmacokinetic data for three radiopharmaceutical agents taken into Phase I clinical testing by BMS Medical Imaging. This scaling was used to predict human pharmacokinetics and compared to values measured in clinical studies. Data from three medical imaging programs, Oncology tumor agent (DPC-A80351), Thrombus agent (DMP-444) and Infection agent (RP-517) were assessed for their predictive accuracy of allometric scaling from pre-clinical models to human. The animal models varied for the Oncology (mouse, dog, and non-human primate), Thrombus (rabbit, dog, and non-human primate) and Infection (guinea pig, rabbit, and non-human primate) programs.

Blood clearance (CL), terminal half-life (t½) and volume of distribution (Vd_{SS}) were determined for each animal model and plotted through allometric scaling without correction factors to predict human pharmacokinetics. Allometric scaling of animal

pharmacokinetic parameters achieved a prediction of the human pharmacokinetic parameter within 13 to 109% of the observed values. This prediction was further improved by adjusting for plasma protein binding of the drug, and achieved an estimate within 5 to 57% of the clinically observed values. Since the parent compound was the dominant species (>95%) in the circulation for all three agents, metabolic stability was not used as a correction factor. Based on the human dose calculated from allometric scaling that would be required to achieve the same drug exposure that provided scintigraphic images in the animal models, the amount of drug administered in the clinical trials should have been, and was, sufficient for imaging.

In conclusion, the allometric scaling method corrected for plasma protein binding yielded a mathematical formula that in most cases reasonably predicted human pharmacokinetics from administration of the radiopharmaceutical imaging agent in a minimum of three animal models. This method will provide an additional tool to better predict the first efficacious and safe dose in human for novel Medical Imaging radiopharmaceuticals.

3.2 Introduction

The following sections provide a brief background on the three BMS Medical Imaging drugs evaluated for allometric scaling prediction in this chapter. Understanding the disease target and mechanism of action of each compound is important when evaluating the pharmacokinetics of the drug and interpreting the results.

3.2.1 DPC-A80351

^{111}In - DPC-A80351 is a selective ligand that binds to the avß3 receptor. The $a_v ß_3$ integrin adhesion receptor is present on angiogenic blood vessels in tissues and tumors (Brooks *et al., 1994*). It interacts with a wide variety of extracellular matrix components and allows vascular cells to invade tissues and form capillary blood vessels (Varner *et al., 1995;* Brooks *et al., 1996*). An elevated level of expression of the integrin $a_v ß_3$ on tumor-associated versus normal blood vessels makes this an attractive target to image tumors.

3.2.2 DMP-444

Tc-99m - DMP-444 binds to the glycoprotein IIb/IIIa receptor on activated platelets with high affinity and specificity (Barrett *et al*., 1996). Activated platelets play an integral role in platelet aggregation and thrombus formation (Plow *et al*., 1987). Deep vein thrombosis is the result of a hypercoagulable state coupled with a period of stasis occurring in a low sheer environment. The end result is the formation of a fibrin rich thrombus that also contains some platelets and erythrocytes. In contrast, an arterial thrombus is the result of the rupture of an atherosclerotic plaque occurring under high sheer conditions resulting in the formation of a platelet rich thrombus. Venous and arterial thrombus formation are common and potentially life-threatening events. The binding of DMP-444 to activated platelets provides the opportunity to image this thrombus.

3.2.3 RP-517

Tc-99m - RP-517, is a ligand for the LTB-4 receptor found on activated neutrophils (van Eerd *et al*., 2003; Tager *et al*., 2003). Activated neutrophils are found at sites of inflammation occurring in response to tissue damage. This tissue damage can result from microbial invasion, auto-immune processes, neoplasms, ischemia, tissue or organ allograft rejection, or such external influences such as heat, cold, radiant energy, chemical stimuli or mechanical trauma. Imaging of RP-517 therefore provides an opportunity to non-invasively detect sites of inflammation/infection.

3.3 Materials and Methods

3.3.1 Animal models

The programs and species evaluated in each program are listed in Table 3.1. The species, other than non-human primate, were selected based on the animal model developed to study the disease-state targeted for each program. The Institutional Animal Care and Use Committee (IACUC) approved all experiments conducted with animals for each of the programs.

Table 3.1 Number of pre-clinical animals and human subjects used for allometric scaling in each Medical Imaging program.

Species/Program	DPC-A80351	DMP-444	RP-517
Mouse	**24**		
Guinea Pig			**4**
Rabbit		**3**	**4**
Dog	**4**	**4**	
Primate	**4**	**5**	**4**
Human	**4**	**20**	**6**

3.3.1.1 DPC-A80351

Mouse- The c-Neu Oncomouse® is a spontaneous tumor bearing model that carries an activated c-Neu oncogene driven by a mouse mammary tumor virus (MMTV) promoter. Transgenic mice uniformly expressing the MMTV/c-neu gene develop mammary adenocarcinomas (4 to 8 months postpartum) that involve the entire epithelium in each gland.

Dog- Canines used for blood pharmacokinetics were normal beagles and one adenocarcinoma tumor-bearing mongrel.

Non-Human Primates- Four male Rhesus Monkeys (Macaca mulatta) were used for evaluation of blood pharmacokinetics.

Human subjects- Pharmacokinetic analysis was conducted on biological samples from cancer patients (n=4) enrolled in the DPC-A80351-101 Oncology Phase I clinical trial.

3.3.1.2 DMP-444

Rabbit- A rabbit carotid injury model was used for blood collection and pharmacokinetic analysis. Male rabbits were anesthetized and the carotid artery stimulated with a 1m Amp current for 20 minutes followed by test article administration.

Dog- Deep-vein thrombosis (DVT) induced dogs were used for blood kinetic studies. Canine beagles were anesthetized with 35 mg/kg sodium pentobarbital, the jugular vein isolated, a balloon catheter inserted and inflated, and thrombin infused for clot formation.

Non-Human Primates- Normal male Rhesus monkeys were used for evaluation of blood pharmacokinetics.

Human subjects- Normal subjects enrolled in Phase I clinical trials were assessed for blood pharmacokinetics.

3.3.1.3 RP-517

Guinea pigs- A guinea pig peritonitis model was used for blood pharmacokinetics. Guinea pigs were anesthetized i.m. with a 2:1 mixture of ketamine/xylazine. A #10 trochar needle was used to introduce a 2 inch piece of umbilical string immersed in a 6% sodium caseinate solution into the right flank. The placement of the immersed string served as the focal site for white blood cell recruitment over eighteen hours.

Rabbits- An e. Coli model of infection was used for blood kinetic evaluation. The rabbit thigh was infected with e. Coli and 24 hrs later the test agent was administered.

Non-Human Primates- Normal Rhesus monkeys were used for evaluation of blood pharmacokinetics.

Humans subjects- Normal subjects enrolled in Phase I clinical trials were assessed for blood pharmacokinetics.

3.3.2 Species Dosing

DPC-A80351, DMP-444 and RP-517 were administered intravenously to animal models and humans based on body weight according to Table 3.2.

Table 3.2 Intravenous dose of DPC-A80351, DMP-444 and RP-517 administered to animal models and humans.

Compound/ Species	**Dose mCi/kg**	**Body Weight (kg)**
DPC-A80351		
Mouse	2.0	0.027
Dog	1.0	8.0
Primate	0.070	13.0
Human	0.39	70
DMP-444		
Rabbit	1.0	2.8
Dog	1.0	9.6
Primate	1.0	11.6
Human	0.133	70
RP-517		
Guinea Pig	0.8	0.5
Rabbit	1.0	2.2
Primate	1.0	15.2
Human	0.357	70

3.3.3 Scintigraphic Imaging

In-house scintigraphic images were taken with a gamma camera (Park Isocam II, Park Medical Systems, Lachine, Quebec) following administration of the test agent to give a qualitative view of the distribution pattern and excretion route of the drug. Human images were collected with various models of clinical gamma camera's following GLP (Good Laboratory Practice) procedures.

3.3.4 Pharmacokinetic analysis

Blood samples were collected in anticoagulant from all species between 0-168 hrs post-injection for counting radioactivity at time-points selected according to the protocol design. An additional aliquot of blood was also centrifuged (2000xg, 15 min) to obtain plasma for plasma protein binding analysis and metabolic profiling. Blood samples were assayed for radioactivity using an LKB gamma counter (Wallac Inc, Gaithersburg, MD). Aliquots were assayed in triplicate for blood. Results from each sample replicate were averaged and concentrations calculated using the following equation:

Radioactivity (µCi) = (Sample counts [counts per minute])/counter efficiency) / ($2.22x10^6$ dpm)

Sample concentrations (uCi/mL) were corrected for isotope decay and adjusted for total volume collected at each time-point using a customized excel spreadsheet. This data was then entered into WinNonlin^{TM} Professional software (Pharsight Corp., Mountain View, CA) and blood pharmacokinetics analyzed (Clearance of drug from the blood (CL), Volume of distribution at steady state (Vdss), and terminal elimination half-life (t½)). Blood clearance is determined by dividing the dose by the area under the curve (AUC) which is calculated from zero to infinity using a linear trapezoidal method. Calculation of the AUC from time zero to the last blood point collected should be at least 80% of the AUC when compared to the AUC calculated from zero to infinity. This is important to ensure the AUC value used in the calculation of clearance represents the majority of the blood exposure. Terminal elimination half-life was calculated using the last 2-4 blood

points depending on the r-squared fit of the line and the inflection points between the distribution and elimination phase of the blood curve. This defines the two-compartment model that was used for all analyses. All species except mouse and guinea pig had full blood curves collected from each animal/human. Mice and guinea pigs do not have sufficient blood volume to collect enough timepoints for a full kinetic curve. Pharmacokinetic parameters were calculated for each subject and reported as average ± standard deviation (SD).

3.3.5 Plasma protein binding

The Centrifree® Ultrafiltration Device (Millipore, Bedford, MA) was used to separate free from protein bound drug (Figure 3.1). This system uses centrifugation through a 30,000 molecular weight cutoff membrane to separate protein bound from unbound drug. The device is accurate, reproducible and has low non-specific binding for the compounds tested.

Figure 3.1 Centrifree® Ultrafiltration Device

For each sample collected for protein binding analysis, four aliquots (0.025 ml) of plasma were transferred to separate polypropylene tubes for counting using an LKB gamma counter (Perkin Elmer/Wallac, Gaithersburg, MD). An aliquot (0.3 ml) of plasma was transferred to a Centrifree® micropartition cartridge (n=4) and centrifuged at 2000 x g for 11 minutes at RT. Following centrifugation, 0.025 ml aliquots (n=4) of filtrate were transferred to polypropylene tubes for gamma counting. The compound was also diluted in saline (~2μCi/ml) and assayed to determine non-specific binding.

The percent of compound bound to plasma proteins was calculated using the following equation:

$$\% \text{ Bound} = \frac{\text{Compound Total - Compound Unbound (filtrate)}}{\text{Compound Total}} \times 100$$

Compound total is radioactivity (dpm) in 0.025ml of sample before ultrafiltration and Compound unbound is radioactivity (dpm) in 0.025ml of filtrate. Data are reported as the mean ± SEM.

3.3.6 Metabolic Stability analysis

Blood samples (0.5 mL) were treated with acetonitrile (2.0 mL) to precipitate plasma proteins. Following centrifugation at 2000 x g for 15 minutes, supernatants were transferred to clean test tubes and dried under nitrogen at 37°C. An aliquot of the test compound was also extracted to ensure the procedure did not cause any compound degradation.

For high-pressure liquid chromatography (HPLC) analysis, 100 µL was injected for each sample. Reverse phase HPLC analysis of plasma was conducted using a Gamma Ram radioactivity detector system (IN/US Systems, Inc., Tampa, FL) with a 0.1 mL flow cell set at 10-500 channel range, and analog output of 7000. A Hewlett Packard 1100 multisolvent HPLC delivery system (Hewlett Packard, Burlington, MA) and a Multichrom data collection system (Thermo Lab Systems, Manchester, UK) were used. HPLC conditions for the three programs are listed in Table 3.3.

Table 3.3 HPLC conditions for Metabolic Stability analyses

	DPC-A80351	DMP-444	RP-517
Column	Zorbax C-18, 25cm	Zorbax C-18, 25cm	Zorbax C-18, 25cm
Temperature (°C)	Ambient	50	Ambient
Flow (mL/min)	1	1	1
Mobile Phase A	25mM NH4 acetate, pH=7.4	25mM NaPo4, pH=8.0	25mM NaPo4, pH=6.0
Mobile Phase B	100% Acetonitrile	100% Acetonitrile	100% Acetonitrile
HPLC Gradient	Time(min) %B 0 2 25 20 26 60 35 60 36 2 45 2	Time(min) %B 0 8 35 14 38 50 38 8	Time(min) %B 0 0 20 75 30 75 31 0

3.3.7 Allometric scaling

Allometric scaling employs log transformation of body weight and pharmacokinetic parameters to extrapolate from animal models to humans. The following equation defines allometric scaling:

$$Y = aW^b$$

Y = physiological parameter (CL, t½, Vd_{SS})

a = allometric coefficient

W = body weight

b = allometric exponent

The equation can also be expressed as:

$$Y = \log a + b \log W$$

(a = y intercept, b = slope)

Each species body weight versus the pharmacokinetic parameter measured was plotted on a log-log scale. The human estimate is then determined through extrapolation of the best-fit line drawn through the other species. In the case of clearance and volume of distribution where values are expressed on a kilogram (kg) basis, the human estimate is divided by an average human weight of 70 kg to give the result on a per kg basis.

When the plasma protein binding was used as a correction factor each pharmacokinetic parameter within species was divided by the percent free fraction and re-plotted on a log-log scale. These adjusted points were then used to extrapolate to the human free fraction estimate. The measured human protein binding was then used to adjust the estimated human free fraction back to a total value.

3.4 Results

3.4.1 Pharmacokinetic

Frequent blood sampling was performed in a number of different species (mouse, rabbit, guinea pig, dog, non-human primate and human) following radioligand (DPC-A80351, DMP-444 and RP-517) administration. Radioactivity in blood was determined by gamma counting. Using customized excel spreadsheets radioactivity counts were decay corrected back to the time of injection and expressed as uCi/ml blood. Using the blood time-activity curves and WinNonlin^{TM} Professional software (Pharsight Corp., Mountain View, CA), pharmacokinetic parameters were determined and results are listed in Table 3.4. For example, DPC-A80351 was administered to a 13-kg primate at 0.07uCi/kg. Blood was collected at 2, 5 15, 30, 45, 60, 90 and 120 minutes post dose and counted for radioactivity. The rate of DPC-A80351 clearance from the blood is calculated (0.37 mL/min/kg) as well as terminal half-life (40.1 min), which is the time it takes the drug concentration to decrease by half once steady state is achieved. The volume of distribution into body water is also calculated (0.15 L/kg) to give an idea of the extent the compound distributes out of the vasculature into extracellular or intercellular water.

Table 3.4 Pharmacokinetic results of DPC-A80351, DMP-444 and RP-517 following I.V. administration in pre-clinical models and humans.

Compound/ Species	**Dose mCi/kg**	**Body Weight (kg)**	**t1/2 (terminal)**	**CL (mL/min/kg)**	**Vdss (L/kg)**
DPC-A80351			(minutes)		
Mouse	2.0	0.027	21.7 ± 7.6	6.12 ± 0.86	3.76 ± 1.74
Dog	1.0	8.0	21.8 ± 0.1	6.51 ± 1.34	6.0 ± 0.35
Primate	0.070	13.0	40.1 ± 9.9	0.37 ± 0.08	0.15 ± 0.05
Human	0.39	70	17.1 ± 4.0	0.43 ± 0.01	0.43 ± 0.08
DMP-444			(hr)		
Rabbit	1.0	2.8	12.3 ± 0.1	0.41 ± 0.08	0.13 ± 0.05
Dog	1.0	9.6	16.5 ± 4.9	2.33 ± 0.33	0.25 ± 0.05
Primate	1.0	11.6	19.9 ± 3.9	0.11 ± 0.01	0.20 ± 0.01
Human	0.133	70	17.9 ± 3.2	0.22 ± 0.03	0.32 ± 0.05
RP-517			(hr)		
Guinea Pig	0.8	0.5	2.3	0.89	0.13
Rabbit	1.0	2.2	2.7 ± 0.4	2.6 ± 0.5	0.37 ± 0.09
Primate	1.0	15.2	7.1 ± 0.8	0.44 ± 0.08	0.18 ± 0.03
Human	0.357	70	16.7 ± 9.0	0.40 ± 0.22	0.58 ± 0.31

t1/2 (terminal)= Terminal half-life; CL=Blood clearance; Vd_{SS} =Volume of distribution at steady state. Values are expressed as mean ± SD (standard deviation)

The pharmacokinetics for these agents showed a range of characteristics. These included a short half-life for DPC-A80351 in all species versus DMP-444 that had a long half-life and RP-517 that had a half-life that was strongly species dependent. DPC-A80351 had a greater range of both clearance and volume of distribution between the species than either of DMP-444 or RP-517 which correlates with the extent of protein binding in each species as discussed in section 3.4.2. These differences provide a good opportunity to examine the usefulness of allometric scaling in varied radiopharmaceutical imaging agents.

3.4.2 Plasma Protein Binding

Plasma protein binding was determined from *in vivo* blood samples taken 15 minutes following radioligand administration. Bound and free ligand were separated by centrifugation through a molecular weight cut-off filter. Plasma protein binding results are shown in Table 3.5. DMP-444 was moderately protein bound in rabbits, primates and humans but showed lower binding in the dog. In contrast, DPC-A80351 showed low protein binding in mice and dogs but considerably higher protein binding in the primate and human. Unfortunately data was only available for RP-517 protein binding in the rabbit.

Table 3.5 *In vivo* Plasma Protein Binding for species at 15 minutes post-injection for each Medical Imaging program.

Species/Program	**DMP-444**	***RP517**	**DPC-A80351**
Mouse	-	-	28.4 ± 8.3
Guinea Pig	-	NA	-
Rabbit	70.0 ± 3.9	32.0 ± 12.1	-
Dog	40.9 ± 2.0	-	13.0 ± 1.1
Primate	83.0 ± 4.7	NA	78.4 ± 3.4
Human	83.0 ± 0.6	NA	83.9 ± 5.7

*Plasma protein binding assessed in rabbit only

3.4.3 Metabolic Stability

In vivo stability was determined by HPLC separation and radiodetection of blood samples taken following *in vivo* administration. Results for each of the compounds tested are listed in Table 3.6. Stability of all compounds in all species tested was > 95%

radiochemically pure up to 15 minutes post-injection. Blood samples analyzed at later times were below the limit of radiochemical detection for 1% metabolites.

Table 3.6 *In vivo* blood stability through 15 minutes post-injection for species in each Medical Imaging program.

% Radiochemical purity

Species/Program	**DMP-444**	**RP-517**	**DPC-A80351**
Mouse	-	-	> 95
Guinea Pig	-	> 95	-
Rabbit	> 95	> 95	-
Dog	> 95	-	> 95
Primate	> 95	> 95	> 95
Human	> 95	> 95	> 95

3.4.4 Scintigraphic Imaging

Scintigraphic images were taken with a gamma camera following administration of the test agent to give a qualitative view of the distribution pattern and excretion route of the drug. Representative images of non-human primate and one other species from each program are shown in Figures 3.2-3.7. Figure 3.2 and Figure 3.3 present mouse and primate images administered DPC-A80351, respectively. Notice the high uptake in the mouse tumors.

0.5 hr Post Injection **1 hr Post Injection** **2 hr Post Injection**

Figure 3.2 Representative scintigraphic images of DPC-A80351 (40 mCi/kg) in c-*neu* Oncomouse® over 2 Hours

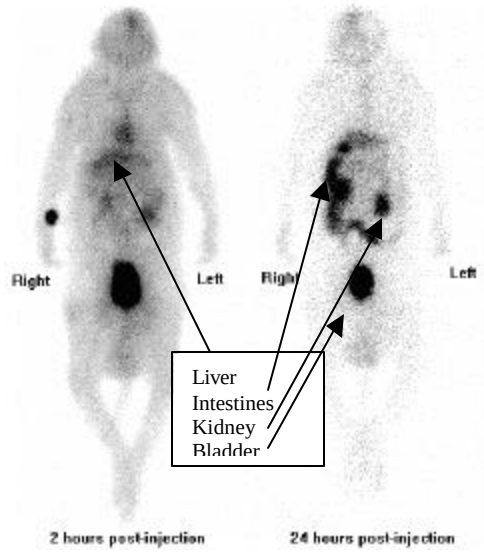

Figure 3.3 Representative whole-body anterior images of monkey at two hours and 24 hours after the administration of 0.5 mCi /kg DPC-A80351.

Both images show a pattern of predominantly renal excretion with some hepatobiliary clearance in the primate. Previous studies have shown a similar pattern of tissue distribution and renal clearance in the c-neu Oncomouse. (Onthank *et al*., 2004 – Appendix I).

Figure 3.4 and Figure 3.5 represent canine and primate images administered DMP-444, respectively. Images show a mixture of renal and hepatobilary clearance in both species. Notice the high uptake in the thrombosis induced in the canine carotid arteries of the neck.

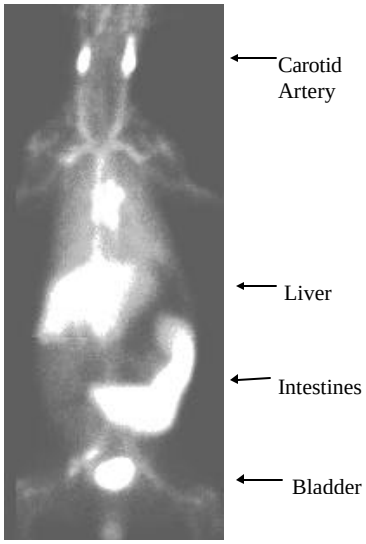

Figure 3.4 Representative scintigraphic image of the canine deep vein thrombosis (DVT) model 60 minutes post-injection following i.v administration of 0.3 mCi/kg DMP-444.

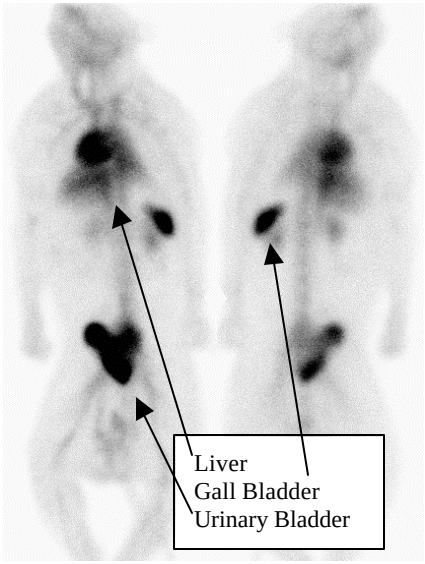

Figure 3.5 Typical whole-body image of rhesus monkey administered DMP 444 at 1 mCi/kg,i.v. Depicted are the anterior (left) and posterior (right), whole body images at 60 min postinjection.

DMP-444 is excreted both renally and hepatobiliary while RP-517 is hepatobiliary cleared. Figure 3.6 and Figure 3.7 show representative images of rabbit and primate following administered of RP-517, respectively. Both images show predominantly hepatobiliary clearance with no visualization of the kidneys. Notice the high uptake in focal infection of the thigh.

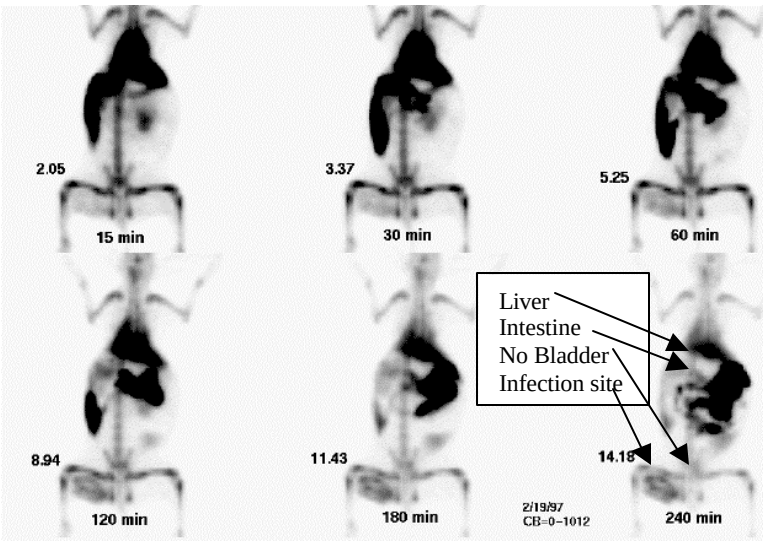

Figure 3.6 Image of RP517 in the Rabbit e. Coli model of infection. RP517 was administered at a dose of 1 mCi/kg,i.v. and uptake monitored over a period of 4 hr postinjection.

Figure 3.7 Representative scintigraphic image of a non-human Primate following i.v. administration of 0.6 mCi/kg RP-517. Images were taken at 0.5, 1 and 4hr post-injection.

Each compound exhibits a good pharmacokinetic profile with respect to the clearance route from the body that allows diagnostic imaging of the intended target. Similar distribution and clearance patterns seen in primates were observed in humans for all compounds. These three radiopharmaceuticals provide a range of excretion patterns to assess how well allometric scaling predicts for different routes of excretion.

3.4.5 Allometric Scaling

Allometric scaling from animals to human for blood clearance, half-life and volume of distribution was conducted for DPC-A80351, DMP-444 and RP-517. Predicted values in the human, before and after applying plasma protein binding correction, were compared to the observed values. The percent error was then calculated between the observed and predicted values.

3.4.6 Blood Clearance

Blood clearance (CL) of DPC-A80351 for each animal model was plotted through allometric scaling pre (Figure 3.8) and post (Figure 3.9) correction for plasma protein binding to predict for human clearance. The extrapolated line fit (R^2) was better when corrected for protein binding and the prediction of blood clearance improved from 109% to 4.7% of the observed value (Table 3.7).

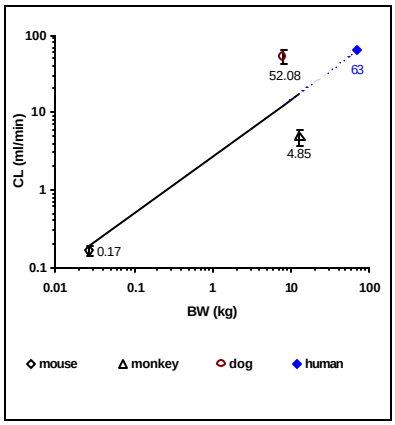

Estimated Human CL=	**0.90**	**ml/min/kg**
CL=a*BWb, a=	**2.69**	
b=	**0.74**	
R2=	**0.78**	

Figure 3.8 Allometric scaling of Blood Clearance for DPC-A80351.

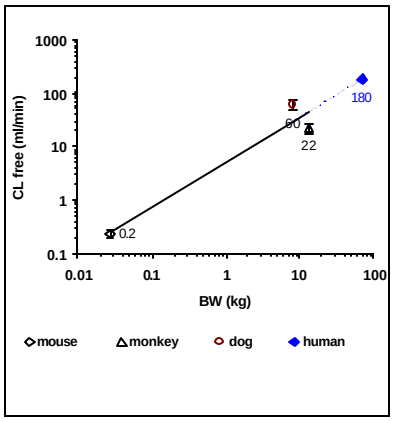

Estimated Human CL=	**0.41**	**ml/min/kg**		
CL free=a*BWb, a=	**5.07**			
b=	**0.84**			
R2=	**0.94**			
	Mouse	**Dog**	**Monkey**	**Human**
Fraction Unbound (fu)	**0.716**	**0.87**	**0.216**	**0.161**

Figure 3.9 Allometric scaling of Blood Clearance for DPC-A80351 corrected for Plasma Protein Binding

Table 3.7 Predicted Versus Observed Clearance in Humans Using Allometric Scaling and Correction Factors.

Drug	**Observed CL (ml/min/kg)**	**Predicted CL Pre-Correction (ml/min/kg)**	**% Error Pre-Correction**	**Predicted CL Post-Correction (ml/min/kg)**	**% Error Post-Correction**	**Species used**
DPC-A80351	0.43 ± 0.01	0.90	**109**	0.41	**4.7**	m, d, rhmk
DMP-444	0.22 ± 0.03	0.39	**77**	0.24	**9.0**	rab, d, rhmk
RP-517	0.40 ± 0.22	0.45	**12.5**	0.45	**12.5**	gp,rab, rhmk

m = mouse, r = rat, gp = guinea pig, d = dog, rab = rabbit, rhmk = rhesus monkey

% Error = (observed-predicted)*100/observed

Similarly, blood clearance of DMP-444 for each animal model was plotted through allometric scaling pre (Figure 3.10) and post (Figure 3.11) correction for plasma protein binding to predict for human clearance. The extrapolated line fit (R^2) was better when corrected for protein binding and the prediction of blood clearance improved from 77% to 9.0% of the observed value (Table 3.7).

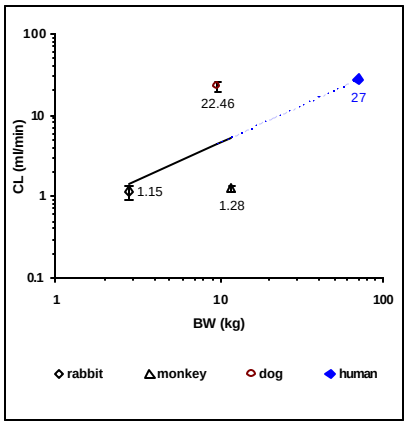

Estimated Human CL=	**0.39**	**ml/min/kg**
CL=a*BWb, a=	**0.55**	
b=	**0.92**	
R2=	**0.18**	

Figure 3.10 Allometric scaling of Blood Clearance for DMP-444.

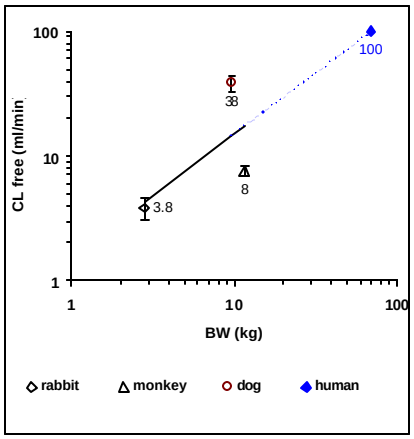

Estimated Human CL=	**0.24**	**ml/min/kg**		
CL free=a*BWb, a=	**1.59**			
b=	**0.97**			
R2=	**0.41**			
	Rabbit	**Dog**	**Monkey**	**Human**
Fraction Unbound (fu)	**0.3**	**0.59**	**0.17**	**0.17**

Figure 3.11 Allometric scaling of Blood Clearance for DMP-444 corrected for Plasma Protein Binding

Blood clearance of RP-517 for each animal model was plotted through allometric scaling pre (Figure 3.12) and post (Figure 3.13) correction for plasma protein binding to predict for human clearance. The corrected clearance values reflected the assumption that protein binding was the same in all species and therefore changed the scale of the plots, however resulted in the same values. The predicted clearance was within 13% of the observed, which is excellent, however may have improved as it did in the other two programs if protein binding data was available (Table 3.7).

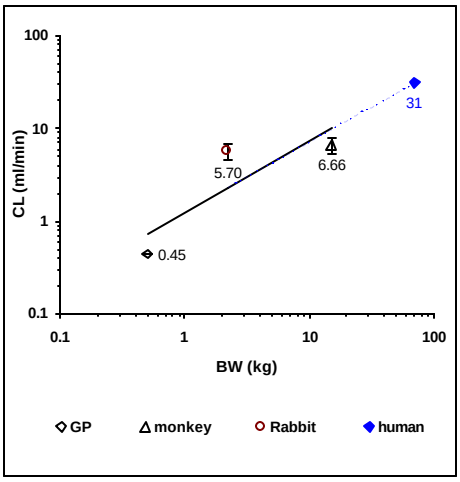

Estimated Human CL=	**0.45**	**ml/min/kg**
CL=a*BWb, a=	**1.26**	
b=	**0.76**	
R2=	**0.73**	

Figure 3.12 Allometric scaling of Blood Clearance for RP-517.

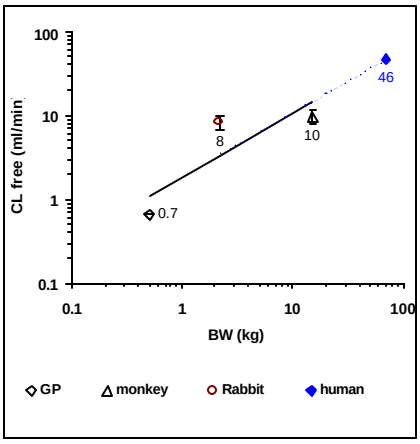

Estimated Human CL=	**0.45**	**ml/min/kg**		
CL free=a*BWb, a=	**1.26**			
b=	**0.76**			
R2=	**0.73**			
	GP	**Rabbit**	**Monkey**	**Human**
Fraction Unbound (fu)	**0.68**	**0.68**	**0.68**	**0.68**

Figure 3.13 Allometric scaling of Blood Clearance for RP-517 corrected for Plasma Protein Binding

3.4.7 Half-life

Terminal half-life of DPC-A80351 for each animal model was plotted through allometric scaling pre (Figure 3.14) and post (Figure 3.15) correction for plasma protein binding to predict for human. The extrapolated line fit (R^2) didn't improve when corrected for protein binding, however the prediction of half-life improved from 96% to 25.7% of the observed value (Table 3.8).

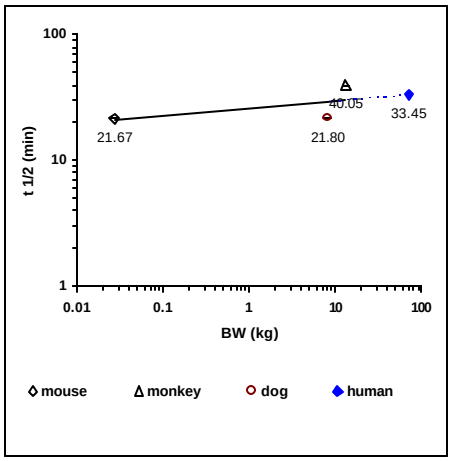

Estimated Human t½=	**33.45**	**minutes**
t½=a*BWb, a=	**26.12**	
b=	**0.06**	
R2=	**0.32**	

Figure 3.14 Allometric scaling of terminal half-life (t½) for DPC-A80351.

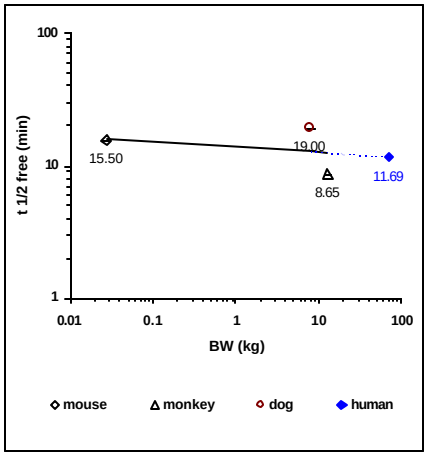

Estimated Human t½=	**21.49**	**min**		
t½ free=a*BWb, a=	**13.85**			
b=	**-0.04**			
R2=	**0.11**			
	Mouse	**Dog**	**Monkey**	**Human**
Fraction Unbound (fu)	**0.716**	**0.87**	**0.216**	**0.161**

Figure 3.15 Allometric scaling of terminal half-life (t½) for DPC-A80351 corrected for Plasma Protein Binding

Table 3.8 Predicted Versus Observed Half-life in Humans Using Allometric Scaling and Correction Factors.

Drug	Observed T½	Predicted T½ Pre-Correction	% Error Pre-Correction	Predicted T½ Post-Correction	% Error Post-Correction	Species used
DPC-A80351	17.1 ± 4.0 (min)	33.5 (min)	**96**	21.5 (min)	**25.7**	m, d, rhmk
DMP-444	17.9 ± 3.2 (hr)	32.2 (hr)	**80**	16.0 (hr)	**10.6**	rab, d, rhmk
RP-517	16.7 ± 9.0 (hr)	10.9 (hr)	**34.7**	10.9 (hr)	**34.7**	gp, rab, rhmk

m = mouse, r = rat, gp = guinea pig, d = dog, rab = rabbit, rhmk = rhesus monkey
% Error = (observed-predicted)*100/observed

Similarly, half-life of DMP-444 for each animal model was plotted through allometric scaling pre (Figure 3.16) and post (Figure 3.17) correction for plasma protein binding to predict for human. Although the extrapolated line fit (R^2) also didn't improve when corrected for protein binding, the prediction of half-life improved from 80% to 10.6% of the observed value (Table 3.8). Because the non-human primate has similar protein binding as the human, the extrapolated line was skewed toward a better estimate of the human half-life.

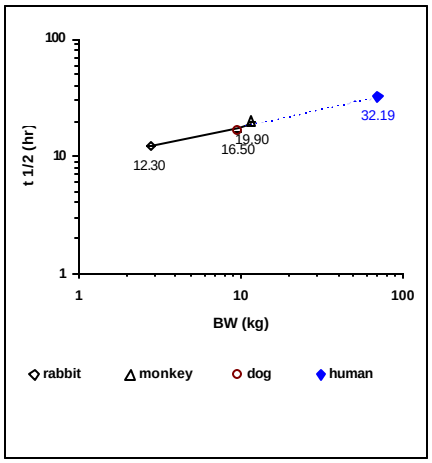

Estimated Human t½=	**32.19**	**hr**
t½=a*BWb, a=	**8.93**	
b=	**0.3**	
R2=	**0.93**	

Figure 3.16 Allometric scaling of terminal half-life (t½) for DMP-444.

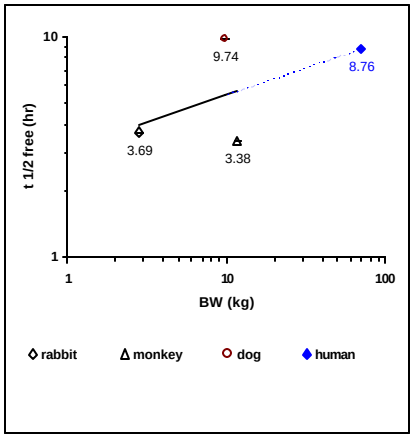

Estimated Human t½=	**16.03**	**hr**		
t½ free=a*BWb, a=	**3.1**			
b=	**0.24**			
R2=	**0.10**			
	Rabbit	**Dog**	**Monkey**	**Human**
Fraction Unbound (fu)	**0.3**	**0.59**	**0.17**	**0.17**

Figure 3.17 Allometric scaling of terminal half-life (t½) for DMP-444 corrected for Plasma Protein Binding

Half-life of RP-517 for each animal model was plotted through allometric scaling pre (Figure 3.18) and post (Figure 3.19) correction for plasma protein binding to predict for human. The corrected half-life values reflected the assumption that protein binding was the same in all species and therefore changed the scale of the plots, however resulted in the same values. The predicted half-life was within 35% of the predicted, which may have improved as it did in the other two programs if protein binding data was available (Table 3.8).

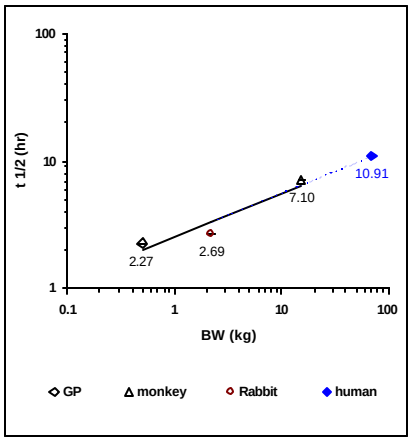

Estimated Human t½=	**10.91**	**hr**
t½=a*BWb, a=	**2.55**	
b=	**0.34**	
R2=	**0.91**	

Figure 3.18 Allometric scaling of terminal half-life (t½) for RP-517.

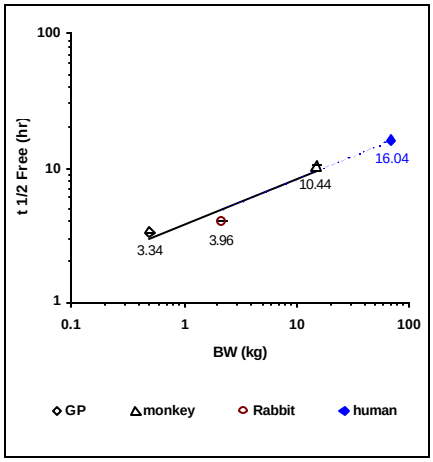

Estimated Human t½=	**10.91**	**hr**		
t½ free=a*BWb, a=	**3.75**			
b=	**0.34**			
R2=	**0.91**			
	GP	**Rabbit**	**Monkey**	**Human**
Fraction Unbound (fu)	**0.68**	**0.68**	**0.68**	**0.68**

Figure 3.19 Allometric scaling of terminal half-life (t½) for RP517 corrected for Plasma Protein Binding

3.4.8 Volume of Distribution

Volume of distribution of DPC-A80351 for each animal model was plotted through allometric scaling pre (Figure 3.20) and post (Figure 3.21) correction for plasma protein binding to predict for human. The extrapolated line fit (R^2) improved when corrected for protein binding, however the prediction of Vd_{SS} changed from 23% to 44.1% of the observed value (Table 3.9). This small change further from the predicted value still results in a reasonable estimate of Vdss.

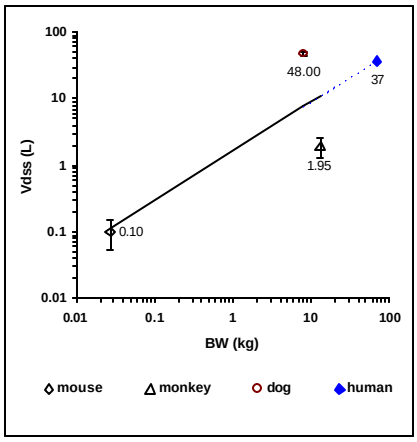

Estimated Human Vdss=	**0.53**	**L/kg**
Vdss=a*BWb, a=	**1.65**	
b=	**0.73**	
R2=	**0.66**	

Figure 3.20 Allometric scaling of Volume of distribution (Vd_{SS}) for DPC-A80351.

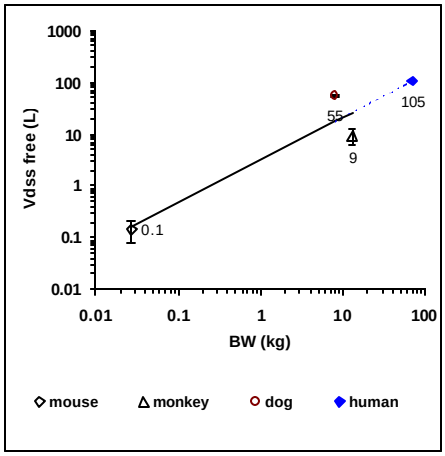

Estimated Human Vdss=	**0.24**	**L/kg**		
Vdss free=a*BWb, a=	**3.11**			
b=	**0.83**			
R2=	**0.87**			
	Mouse	**Dog**	**Monkey**	**Human**
Fraction Unbound (fu)	**0.716**	**0.87**	**0.216**	**0.161**

Figure 3.21 Allometric scaling of Volume of distribution (Vd_{SS}) for DPC-A80351 corrected for Plasma Protein Binding

Table 3.9 Predicted Versus Observed Vdss in Humans Using Allometric Scaling and Correction Factors.

Drug	**Observed Vdss (L/kg)**	**Predicted Vdss Pre-Correction (L/kg)**	**% Error Pre-Correction**	**Predicted Vdss Post-Correction (L/kg)**	**% Error Post-Correction**	**Species used**
DPC-A80351	0.43 ± 0.08	0.53	**23**	0.24	**44.1**	m, d, rhmk
DMP-444	0.32 ± 0.05	0.46	**44**	0.28	**12.5**	rab, d, rhmk
RP-517	0.58 ± 0.31	0.25	**57**	0.25	**57**	gp, rab, rhmk

m = mouse, r = rat, gp = guinea pig, d = dog, rab = rabbit, rhmk = rhesus monkey

% Error = (observed-predicted)*100/observed

Volume of Distribution of DMP-444 for each animal model was plotted through allometric scaling pre (Figure 3.22) and post (Figure 3.23) correction for plasma protein binding to predict for human Vd_{SS}. The extrapolated line fit (R^2) was slightly worse when corrected for protein binding, however the prediction of Vd_{SS} improved from 44% to 12.5% of the observed value (Table 3.9).

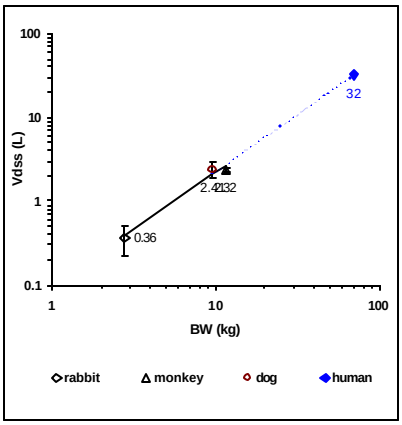

Estimated Human Vdss=	**0.46**	**L/kg**
Vdss=a*BWb, a=	**0.09**	
b=	**1.38**	
R2=	**0.98**	

Figure 3.22 Allometric scaling of Volume of distribution (Vd_{SS}) for DMP-444.

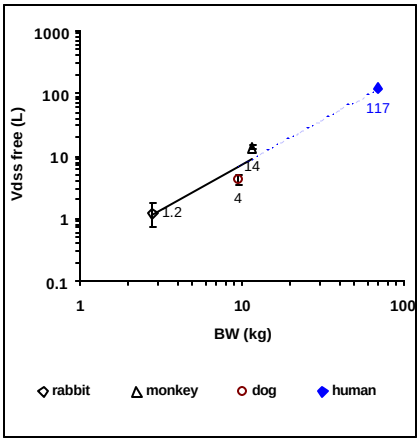

Estimated Human Vdss=	**0.28**	**L/kg**		
Vdss free=a*BWb, a=	**0.26**			
b=	**1.44**			
R2=	**0.85**			
	Rabbit	**Dog**	**Monkey**	**Human**
Fraction Unbound (fu)	**0.3**	**0.59**	**0.17**	**0.17**

Figure 3.23 Allometric scaling of Volume of distribution (Vd_{SS}) for DMP-444 corrected for Plasma Protein Binding

Volume of distribution of RP-517 for each animal model was plotted through allometric scaling pre (Figure 3.24) and post (Figure 3.25) correction for plasma protein binding to predict for human. The corrected Vd_{SS} values reflected the assumption that protein binding was the same in all species and therefore changed the scale of the plots, however resulted in the same values. The predicted Vd_{SS} was within 57% of the predicted, which may have improved as it did in the other two programs if protein binding data was available (Table 3.9).

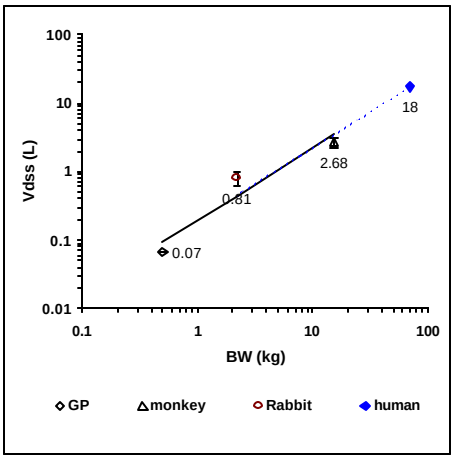

Estimated Human Vdss=	**0.25**	**L/kg**
Vdss=a*BWb, a=	**0.19**	
b=	**1.06**	
R2=	**0.93**	

Figure 3.24 Allometric scaling of Volume of distribution (Vd_{SS}) for RP-517.

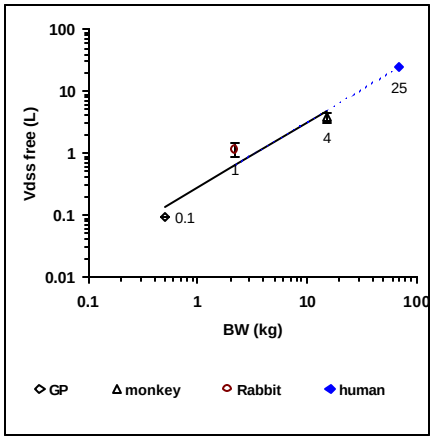

Estimated Human Vdss=	**0.25**	**L/kg**		
Vdss free=a*BWb, a=	**0.28**			
b=	**1.06**			
R2=	**0.93**			
	GP	**Rabbit**	**Monkey**	**Human**
Fraction Unbound (fu)	**0.68**	**0.68**	**0.68**	**0.68**

Figure 3.25 Allometric scaling of Volume of distribution (Vd_{SS}) for RP-517 corrected for Plasma Protein Binding

The pharmacokinetic predictions for humans based on the non-corrected allometric scaling were in the range of 13 to 109% of the measured values. These estimates improved further when values were adjusted for protein binding (5-57% of predicted value). Improvements were most apparent for DPC-A80351, which had a strong species dependency to the protein binding. Smaller effects were present with RP-517 where very limited protein binding data was available.

3.5 Discussion

For the three compounds examined, allometric scaling without correction predicted within 109% (often considerably better) of the measured pharmacokinetic parameters. If these pharmacokinetic parameters were then used for calculating the optimum imaging dose in human, the predicted dose could be 100% different since dose is directly proportional to the change in blood clearance (Dose= Cl x AUC). Allometric scaling corrected for protein binding improves the predicted dose within 13%. In contrast to body weight scaling, the dose to produce the same pharmacokinetic value if scaled on a meter squared body surface area results in a 20–40 fold over-prediction of clearance in the three programs. Whereas body surface area typically reflects differences in metabolism versus differences in body weight and is often used for conversion and calculations in safety toxicology studies, it doesn't appear to work particularly well for predicting pharmacokinetics in these programs.

Plasma protein binding was seen to differ markedly with DPC-A80351 from species to species. Since clearance, distribution and half-life are all dependent on the amount of drug available versus the amount bound, protein binding has the potential to markedly influence predictions from species to species. This was demonstrated by the marked improvement in the prediction of pharmacokinetic parameters by allometric scaling for DPC-A80351 following correction for protein binding. The protein binding

correction had less of an impact on the predictions made for DMP-444. This reflects the smaller range between the different species in protein binding. The minimal impact for RP-517 was expected since the only protein binding value was in the rabbit, therefore, no species selective adjustments were achieved.

If protein binding and/or metabolic stability are not considered when calculating blood clearance, it would not be clear if the drug concentration reflects intact drug or metabolic fragments and to what extend they are bound to plasma proteins. Various combinations of these unknown variables could surely influence interpretation of the pharmacokinetic data. Correcting for pharmacokinetic differences using metabolic stability is difficult when only one or two single time-points are taken early in the distribution phase of the kinetic curve. At the time a blood sample is counted for radioactivity, the counts represent all radioactivity, which includes parent drug and all metabolic fragments. These fragments may also be bound in different amounts to plasma proteins. Since metabolic stability was > 95% radiochemical purity in all species across the programs, there was no need for correction.

The terminal half-life of compound in circulation may be difficult to estimate if blood is not sampled long enough post-injection to capture at least 80% of the total area under the blood concentration-time curve. If multiple blood samples are not collected in the terminal elimination phase to clearly define the slope of the line, the half-life may be over or under estimated. In the current three programs this was not an issue and the results reflected a percent error between predicted and observed values of < 35%.

Another important consideration in allometric scaling is the selection of species used in the analysis. It is not only important to have 2-3 species for accurate predictive scaling, it is also necessary to ensure that species size varies enough in body weight to control the slope of the line for predicting a given pharmacokinetic parameter. All three programs discussed in this chapter had a wide range of weights for the species tested. If the animals used for modeling are all close in body weight, the slope of the line drawn for predicting a 70-kg human could be poorly defined because of a small range of data points and result in a poor prediction as described in chapter one, section 1.1.7. It is important therefore to include a small animal species (i.e. mouse, rat) in the extrapolation, which is typically done for toxicokinetic studies anyway. Recent data published by Tang *et al*, 2005, suggests that certain species or combination of species used in experimental modeling are better for predicting pharmacokinetic parameters than others and note that the number of animals tested within a species can add variability to the extrapolated line fit. In other words, if one or two species in particular have shown previous similarities to human *in vitro* results or the literature has suggested a model that is similar in drug disposition to the human for a similar drug, more emphasis should be placed on this model. Increased replicates or more weighting should also be considered. It is also worth noting that allometric scaling using all species predicted more accurately than estimating from primate alone in all three programs.

Based on the results of the research described in this dissertation, blood clearance in the human can be predicted with reasonable accuracy from animal models using allometric scaling. This does not ensure that the blood exposure of the drug to the target

in humans will be sufficient to deliver enough to bind to the target and elicit a response similar to that observed in the animal models. Thus, the next challenge is to use this data to select a dose that will provide the same binding to the target as observed in the animal models. To accomplish this, it is assumed that the same blood exposure of the compound in the animal models would need to be achieved in humans to obtain similar target uptake. In other words, the total blood exposure (area under the blood concentration-time curve) should be the same in animals as in humans assuming similar interactions between the drug and target are necessary for uptake. If the same blood exposure is required, then the human dose can be calculated using the formula, Dose = Cl x AUC, where Cl is the predicted human clearance and AUC is the area under the curve from the animal model blood concentration-time curves. Based on the average AUC observed for the two disease state animal models in the Oncology program (mouse and dog, 0.33 and 0.15 uCi*min/ml, respectively) the human dose required to achieve the same AUC using the calculated allometric clearance value would be 0.1 uCi/kg. The actual dose administered in the clinical trials was 0.39 uCi/kg which is 3.9 times the dose calculated to successfully deliver enough drug to its target for the expected response. The actual imaging data from the clinical trials suggested limited tumor uptake from the few patients in the trial (n=4), however the tumor size and type may have explained low uptake as opposed to not enough drug delivered. Alternatively, the distribution and number of receptors in the human tumor versus the animal tumor could have been sufficiently different to explain the difference. Similarly, based on the average AUC observed for the two disease state animal models in the Infection program (guinea pig and rabbit, 0.90 and

0.38 uCi*min/ml) the human dose required to achieve the same AUC and using the calculated allometric clearance value would be 0.29 uCi/kg. The actual dose administered in the clinical trials was 0.36 uCi/kg which is 1.2 times the dose calculated to successfully deliver enough drug to its target for the expected response. The Thrombus program showed the predicted human dose was high enough (0.13 uCi/kg) based on the AUC exposure in the dog model (0.43 uCi*min/ml), however 4.4 fold too low based on the AUC exposure in the rabbit model (2.4 uCi*min/ml). These data indicate that human doses administered in the clinical programs were sufficient to deliver enough drug to its target to elicit a response assuming AUC in animal models are predictive of AUC in humans.

Allometric scaling of body weight corrected to free fraction of drug in the blood appears to accurately predict drug clearance and an efficacious dose in human. Direct body weight scaling was mentioned early in the discussion, however other methods that may provide good pharmacokinetic estimates such as allometric scaling of body surface area (BSA) are also applicable. Animal models used for pharmacokinetic analysis are typically smaller than humans and usually have higher metabolic rates. Therefore, body surface area is often used for extrapolation based on the assumption that it corrects for differences in metabolism better than body weight (*Kwiatkowski R., 1999*). If body surface area calculations were used to predict dose in humans in the medical imaging programs, an overestimation of dose would be calculated as mentioned earlier.

The literature reviews many scaling methods for predicting pharmacokinetics as reviewed in chapter one. Often, pharmacokinetic data are compiled from the literature and used to make scaling predictions with minimal, if any, assessment of protein binding or metabolic stability data to help characterize the fate of the drug in circulation. This may be an issue with the various methods that have not optimally predicted pharmacokinetic parameters. Protein binding and metabolic stability results are very important to consider when predicting human pharmacokinetics.

Accurate prediction of blood clearance and volume of distribution in humans for a particular drug is important for calculating the total exposure from a given amount of compound administered. This is essential, when considering selection of the first dose in human, to ensure circulating blood concentrations are safe and at high enough concentrations to target the disease process (Benet *et al.*, 1984). Based on human dose estimates from the allometric scaling, doses administered in the clinical programs were sufficient to deliver enough drug to its target to elicit a response, assuming drug exposure in animal models is the same exposure required in humans. This may be a dangerous assumption considering possible differences in the target, including: receptor density/specificity, morphology and other characteristics that may influence drug targeting, however many of these concerns may be addressed using *in vitro* assay testing. Providing this additional pharmacokinetic information to the regulatory agencies will help support the proposed level of drug for administration. Highly predictive results are expected from animal models not only qualitatively but quantitatively as well. This

continues to be a challenging problem. Humans are highly diverse both biologically and genetically, which makes extrapolation even more difficult.

4. CHAPTER 4

Prediction of "First Dose in Human" for an Atherosclerotic Plaque Targeted Radiopharmaceutical Imaging Agent Based on Allometric Scaling of Pharmacokinetics in Pre-Clinical Animal Models

4.1 Summary

Allometric scaling corrected for plasma protein binding was applied to pharmacokinetic data derived from an atherosclerotic plaque targeted radiopharmaceutical imaging agent, RP845-Tc-99m, currently in development. Blood clearance (CL), terminal half-life (t½) and volume of distribution (Vd_{SS}) were determined for mouse, rat and rabbit, then plotted through allometric scaling without correction factors to predict non-human primate pharmacokinetics. Differences between predicted versus observed non-human primate Cl, t½ and Vd_{SS}, before applying correction factors, were 40%, 52% and 8%, respectively. Following allometric scaling correcting for plasma protein binding, predicted versus observed Cl, t½ and Vd_{SS} results were 12%, 3% and 38%, respectively. Allometric scaling alone predicted non-human primate pharmacokinetics from other animal models within 52% overall, however following correction for free fraction of the drug, predictions achieved an accuracy of < 38% of the observed values. Since blood clearance is considered one of the key parameters in predicting human dose, the improvement from 40% to 12% was significant. The metabolic stability in all species was similar and, therefore, not used as a correction factor.

Mouse, rat, rabbit and non-human primate were then used for allometric scaling with plasma protein binding correction to predict human CL, t½ and Vd_{SS}. The predicted values were 7.6 mL/min/kg, 70.6 minutes and 0.87 L/kg for CL, t½ and Vd_{SS}, respectively. Using the predicted blood clearance in human through allometric scaling, a typical RP845-Tc-99m dose of 25 mCi/subject would be ten times below the dose required to image atherosclerotic plaque in humans based on data from the animal model images. This represents a good example of how predicting accurate blood clearance of a compound in humans through corrected allometric scaling would help evaluate the compound's targeting potential and success of scintigraphic imaging. This information would also help guide structural modifications to optimize pharmacokinetics and provide an indication of the expected compound delivery to the target in clinical trials.

4.2 Introduction

The atherosclerotic plaque-imaging agent is a technetium-99m radiopharmaceutical under development to allow the identification of patients at high risk of coronary events by targeting and imaging atherosclerotic lesions. Atherosclerosis is a disease of blood vessels involving cellular and morphological changes of the vessel wall that may lead to coronary thromboses resulting from rupture of the fibrous cap of the plaque. Literature now supports the concept that the atherosclerotic plaques can undergo continuous and dynamic remodeling and displays considerable metabolic activity (Bentzon *et al*., 2003; Sosnovik *et al*., 2002). This presents opportunities to develop imaging agents that may identify when plaques are at high risk (vulnerable plaques) of rupturing and precipitating acute myocardial infarction or unstable angina. Currently, there are no accurate methods of non-invasively assessing the location or degree of atherosclerotic plaque burden in the coronary vessels.

The vulnerable plaque research project described in this chapter examines the use of allometric scaling corrected for plasma protein binding to better utilize the data available from animal models to predict a safe and efficacious clinical dose. Pharmacokinetic data from three animal models will be used to predict pharmacokinetics in the non-human primate and assessed for accuracy of the prediction. Human pharmacokinetics will then be determined using all the species.

4.3 Materials and Methods

4.3.1 RP845-Tc-99m

RP845-Tc-99m is a low molecular weight, hydrophilic ^{99m}Tc containing chelate administered as a single intravenous dose. A localization sequence in RP845-Tc-99m causes the molecule to be preferentially retained in plaque bearing arterial walls and have low association and rapid clearance from other non-target tissues. These characteristics make it an ideal candidate for an imaging agent.

4.3.2 Animal models

The species evaluated in this program are listed in Table 4.1. The mouse and rabbit are well-defined atherosclerotic plaque models used in the literature and were selected on this basis (Johnson *et al*., 2001; Rosenfeld *et al*., 2000; Johnstone *et al*., 2001; Feldman *et al*., 2001). The rat will be used for toxicology studies and was therefore chosen as the third species used for predicting non-human primate pharmacokinetics. The Institutional Animal Care and Use Committee (IACUC) has reviewed protocol procedures and approved all experiments conducted with animals.

Table 4.1 Pre-clinical animal models used for allometric scaling of RP845-Tc-99m.

Species	**# Animals**
Mouse	3
Rat	3
Rabbit	5
Non-human Primate	1

Mouse- The apolipoprotein E (ApoE) knockout mouse is a model of hypercholesterolemia that develops atherosclerotic lesions in the brachiocephalic artery, the aortic arch and the abdominal aorta. Mice are fed a high-fat diet to accelerate plaque formation and administered test compounds between 37- 41 weeks on diet.

Rat- Normal Sprague-Dawley rats were used for blood pharmacokinetics.

Rabbit- Atherosclerosis was induced in New Zealand White male rabbits (3 kg) with aortic balloon endothelial injury followed by feeding a 0.5% cholesterol diet for 22 weeks.

Non-Human Primate- A male Rhesus Monkey (Macaca mulatta) was used for evaluation of blood pharmacokinetics.

4.3.3 Species Dosing

RP845-Tc-99m was administered as a single, bolus intravenous dose to animals based on body weight according to Table 4.2.

Table 4.2 Intravenous dose of RP845-Tc-99m administered to animal models.

Species	**Dose (mCi/kg)**	**Body Weight (kg)**
Mouse	5.4	0.025
Rat	0.4	0.36
Rabbit	1.3	3.4
Non-human Primate	1.2	5.4

4.3.4 Scintigraphic Imaging

Scintigraphic images were taken with a gamma camera (Park Isocam II, Park Medical Systems, Lachine, Quebec) following administration of the test agent to give a qualitative view of the distribution pattern and excretion route of the drug.

4.3.5 Blood sample collection

Blood samples were collected into sodium heparin anticoagulant from all species between 0-168 hrs post-injection at timepoints selected according to the protocol design. All samples were weighed and assayed for radioactivity. An aliquot of blood was also

centrifuged (2000xg, 15 min) to obtain plasma for plasma protein binding analysis and metabolic profiling.

4.3.6 Pharmacokinetic analysis

Blood samples were assayed for radioactivity using an LKB gamma counter (Wallac Inc, Gaithersburg, MD). Aliquots were assayed in triplicate for all blood samples. Results from each sample replicate were averaged and concentrations calculated using the following equation:

Radioactivity (µCi) = (Sample counts [counts per minute])/counter efficiency) / (2.22×10^6 dpm)

Sample concentrations (uCi/mL) were corrected for isotope decay and adjusted for total volume collected at each timepoint. Blood pharmacokinetic analysis was performed using WinNonlin^{TM} Professional software (Pharsight Corp., Mountain View, CA). Clearance of drug from the plasma (CL), Volume of distribution at steady state (Vdss), and Elimination half-life (t½) were calculated.

4.3.7 Plasma protein binding

For each sample collected for protein binding analysis, four aliquots (0.025 ml) of plasma were transferred to separate polypropylene tubes for counting using an LKB gamma counter (Perkin Elmer/Wallac, Gaithersburg, MD). An aliquot (0.3 ml) of plasma was transferred to a Centrifree® micropartition cartridge (n=4) and centrifuged at 2000 x g for 11 minutes at RT. After centrifugation, 0.025 ml aliquots (n=4) of filtrate were transferred to polypropylene tubes for gamma counting. The compound kit was also diluted in saline (~2μCi/ml) and assayed to determine non-specific binding.

Data Analysis

The percent of compound bound to plasma proteins was calculated using the following equation:

$$\% \text{ Bound} = \frac{\text{Compound Total - Compound Unbound (filtrate)}}{\text{Compound Total}} \times 100$$

Compund total is radioactivity (dpm) in 0.025ml of sample before ultrafiltration and Compound unbound is radioactivity (dpm) in 0.025ml of filtrate. Data are reported as the mean ± SEM.

4.3.8 Metabolic Stability analysis

Blood samples (0.5 mL) were treated with acetonitrile (2.0 mL) to precipitate plasma protiens. Following centrifugation at 2000 x g for 15 minutes, supernatants were transferred to clean test tubes and dried under nitrogen at 37°C. Samples were reconstituted and 100 uL used for high-pressure liquid chromatography (HPLC) analysis,. Reverse phase HPLC analysis of plasma was conducted using a Gamma Ram radioactivity detector system (IN/US Systems, Inc., Tampa, FL) with a 0.1 mL flow cell set at 10-500 channel range, and analog output of 7000. A Hewlett Packard 1100 multisolvent HPLC delivery system (Hewlett Packard, Burlington, MA) and a Multichrom data collection system (Thermo Lab Systems, Manchester, UK) were used. The flow rate through the HPLC column (Zorbax RX-C18, 250 x 4.6 mm) and guard column (Zorbax C18, 12.5 mm x 4.6 mm) was 1 mL/minute. Deproteinized plasma extracts were analyzed using a gradient of 25 mM ammonium acetate/acetonitrile over 30 minutes. The column was equilibrated for 10 minutes with the initial conditions prior to the next injection.

An aliquot of the test compound was also subjected to the extraction procedure and used to determine if HPLC peaks in samples were present in the collected sample or formed during the extraction procedure.

4.3.9 Allometric scaling

Allometric scaling employs log transformation of body weight and pharmacokinetic parameters to extrapolate from animal models to humans. The equation is defined in chapter three, section 3.3.7.

Each species body weight versus the pharmacokinetic parameter measured is plotted on a log-log scale. The non-human primate or human estimate is then determined through extrapolation of the best-fit line drawn through the other species. In the case of clearance and volume of distribution where values are expressed on a kilogram (kg) basis, the non-human primate or human estimate is divided by the body weight to express the result per kg.

When the plasma protein binding was used as a correction factor each pharmacokinetic parameter within species was divided by the percent free fraction and re-plotted on a log-log scale. These adjusted points were then used to extrapolate to the non-human primate or human free fraction estimate. The measured protein binding was then used to adjust the estimated non-human primate or human free fraction back to a total value.

4.4 Results

4.4.1 Pharmacokinetic results

Pharmacokinetic results for RP845-Tc-99m in pre-clinical animal models are presented in Table 4.3.

Table 4.3 Pharmacokinetic results of RP845-Tc-99m following I.V. administration in pre-clinical models. Values are expressed as mean ± SD (standard deviation)

Species	**Dose (mCi/kg)**	**Body Weight (kg)**	**t1/2 (terminal) (minutes)**	**CL (mL/min/kg)**	**Vdss (L/kg)**	**AUC (mCi*min/mL)**
Mouse	5.4	0.025	60.3	7.11	0.58	0.76
Rat	0.39	0.36	66.6 ± 1.2	12.9 ± 0.14	0.96 ± 0.37	0.03
Rabbit	1.3	3.4	106.5 ± 11.4	3.63 ± 0.86	0.50 ± 0.07	0.36
Non-human Primate	1.2	5.4	68.6	8.2	0.66	0.15

t1/2 (terminal)= Terminal half-life; CL=Blood clearance; $V_{D\,ss}$=Volume of distribution at steady state, AUC=Area under the blood concentration-time curve

The pharmacokinetics indicate rapid blood clearance in all species as evident from the short half-life in all species. The volume of distribution suggests hydrophilic characteristics with distribution into extracellular and intercellular compartments. All species except rabbit clear the blood faster than kidney filtration alone, based on the glomerular filtration rates for mouse (14 mL/min/kg), rat (5.2 mL/min/kg), rabbit (3.1 mL/min/kg) and non-human primate (2.1 mL/min/kg), as reported by Davies and co-workers (1993). Hepatobiliary clearance as well as renal clearance is evident in mouse and non-human primate images shown in the scintigraphic images results section.

4.4.2 Plasma Protein Binding

Plasma protein binding results are shown in Table 4.4. Percent bound to proteins was low in all species examined.

Table 4.4 *In vivo* Plasma Protein Binding of RP845-Tc-99m at 15 minutes post-injection in mouse, rat, rabbit and non-human primate.

Species	**% Protein Bound**
Mouse	20.3
Rat	54.1
Rabbit	41.5
Primate	27.3

The *in vitro* binding for human plasma when incubated for 15 minutes was 20.1%. This is similar to the *in vivo* value seen in the NHP and mouse. Previous studies have indicated that *in vitro* values are often comparable to those measured *in vivo.*

4.4.3 Metabolic Stability

In vivo blood stability for each of the compounds tested is listed in Table 4.5. Stability of all compounds within all species was 71-78% parent compound up to 15 minutes post-injection.

Table 4.5 *In vivo* blood stability of RP845-Tc-99m through 15 minutes post-injection in mouse, rat, rabbit and non-human primate.

Species/Program	**% RP845**
Mouse	72
Rat	78
Rabbit	76
Non-human primate	71

Radiochemical purity of RP845 for *in vitro* human plasma determinations at 15 minutes of incubation was 72%. Pharmacokinetic predictions were not corrected for metabolic stability since there was equivalent stability in all species tested.

4.4.4 Scintigraphic Imaging

Scintigraphic images were taken with a gamma camera following administration of the test agent to give a qualitative view of the distribution pattern and excretion route of the drug. Mouse, rabbit and non-human primate images following administration of RP845-Tc-99m are depicted in Figure 4.1, Figure 4.2 and Figure 4.3, respectively.

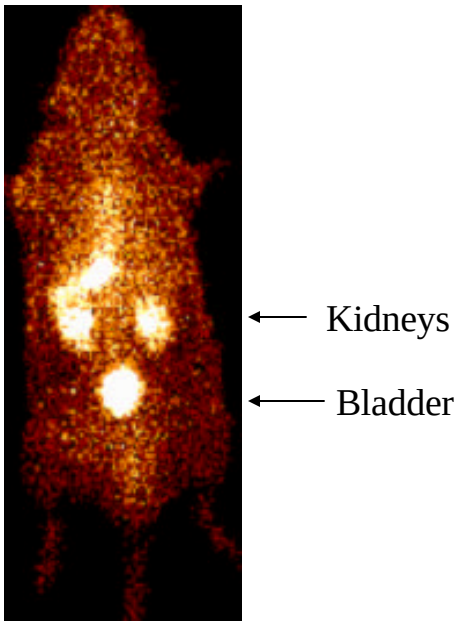

Figure 4.1 Representative scintigraphic image of the ApoE mouse model at 1hr post-injection following i.v administration of 20 mCi/kg RP845-Tc-99m.

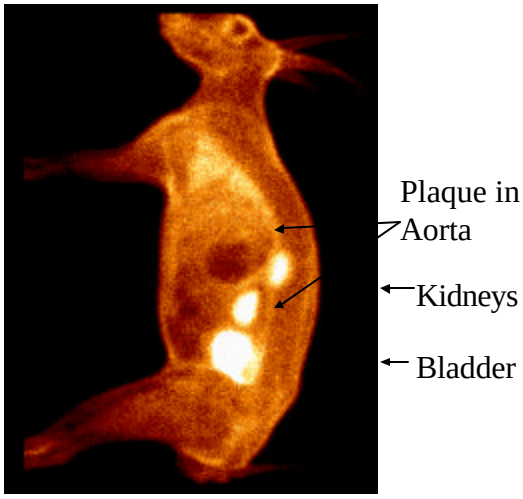

Figure 4.2 Representative scintigraphic image of RP845-Tc-99m at 1 hr post injection in the New Zealand Rabbit plaque model.

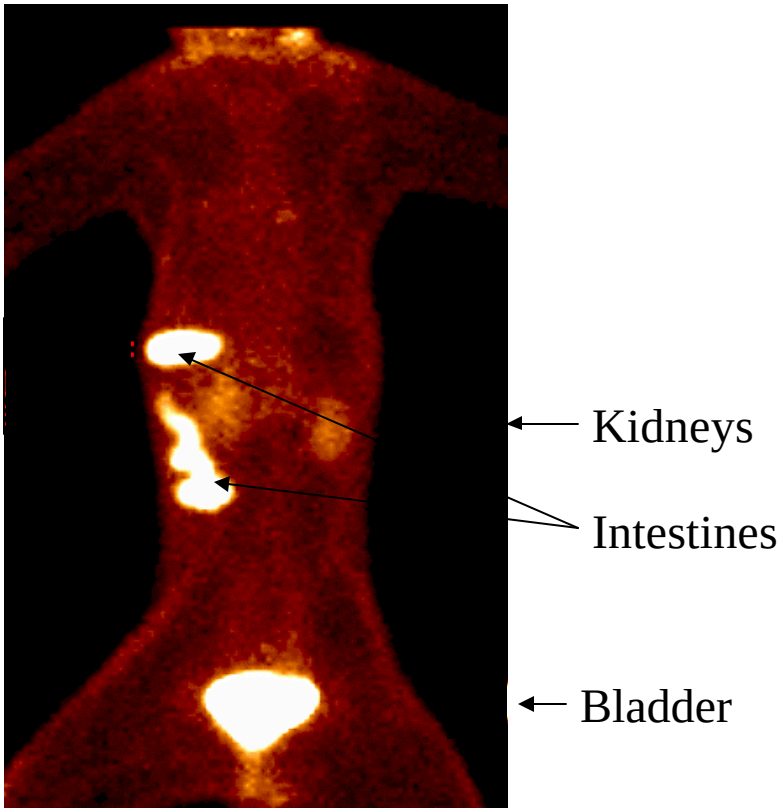

Figure 4.3 Representative whole-body anterior images of a non-human primate at 2hr post-injection of 1.0 mCi /kg RP845-Tc-99m.

RP-845-Tc-99m exhibits an excellent pharmacokinetic profile for an atherosclerotic plaque diagnostic-imaging agent with rapid clearance from the body and predominantly renal excretion. RP-845-Tc-99m does, however, show slight qualitative differences in excretion between the species. Mouse exhibits mainly renal excretion with some evidence of hepatobiliary clearance, rabbit shows primarily renal clearance and non-human primate excretes through both routes. These three models suggest a range of excretion patterns as evident from the blood clearance values and scintigraphic images.

The models provide data to assess how well allometric scaling predicts pharmacokinetics with different routes of excretion in the species.

4.4.5 Allometric Scaling

Allometric scaling for blood clearance, half-life and volume of distribution was calculated for non-human primate using data from the mouse, rat and rabbit (Table 4.6).

Table 4.6 Predicted Versus Observed Pharmacokinetics in Non-Human primate Using Allometric Scaling and Protein Binding Correction.

Parameter	Observed	Predicted Pre-Correction	% Error Pre-Correction	Predicted Post-Correction	% Error Post-Correction	Species used
CL (ml/min/kg)	8.2	4.9	**40**	7.2	**12**	m, r, rab
T1/2 (min)	68.6	104.1	**52**	70.7	**3**	m, r, rab
VDss (L/kg)	0.66	0.61	**8**	0.91	**38**	m, r, rab

m = mouse, r = rat, rab = rabbit
% Error = (observed-predicted)*100/observed

The percent error following correction for plasma protein binding decreased for CL and T½ . In contrast, Vd_{SS} predicted the observed value more accurately before correcting for protein binding. Although the observed values represent data from only one non-human primate, the parameters Cl, T½ and Vdss were all predicted within 38%. Additional non-human primate studies may improve the accuracy of these results.

Allometric scaling of blood clearance in mouse, rat, rabbit and non-human primate was conducted to predict human clearance. Blood clearance of RP845 for each animal model was plotted through allometric scaling pre (Figure 4.4) and post (Figure 4.5) correction for plasma protein binding. Clearance increased slightly following protein binding correction while the line fit remained similar.

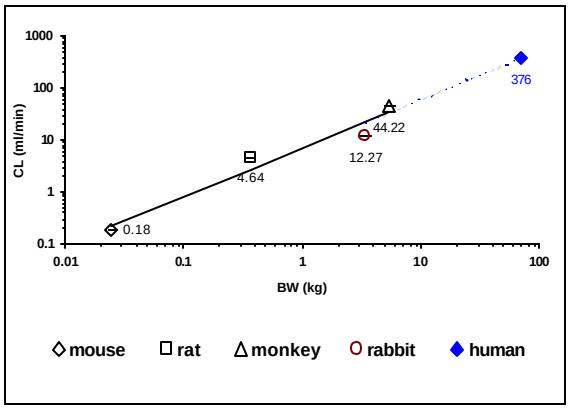

Estimated Human CL=	**5.37**	**ml/min/kg**
CL=a*BWb, a=	**7.03**	
b=	**0.94**	
R2=	**0.95**	

Figure 4.4 Allometric scaling of Blood Clearance for RP845-Tc-99m.

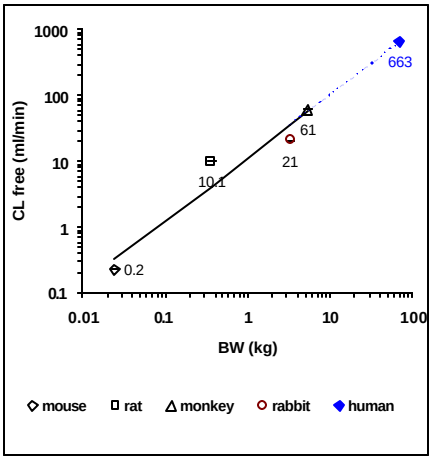

Estimated Human CL=	**7.57**	**ml/min/kg**			
CL free=a*BWb, a=	**11.3**				
b=	**0.96**				
R2=	**0.93**				
	Mouse	**Rat**	**Monkey**	**Rabbit**	**Human**
Fraction Unbound (fu)	**0.797**	**0.459**	**0.727**	**0.585**	**0.8**

Figure 4.5 Allometric scaling of Blood Clearance for RP845-Tc-99m corrected for Plasma Protein Binding

Half-life of RP845 for each animal model was plotted through allometric scaling pre (Figure 4.6) and post (Figure 4.7) correction for plasma protein binding to predict for human. Half-life and line fit decreased following protein binding correction. Rat appeared to have the largest impact on the fit of the line due to the highest protein binding of the species.

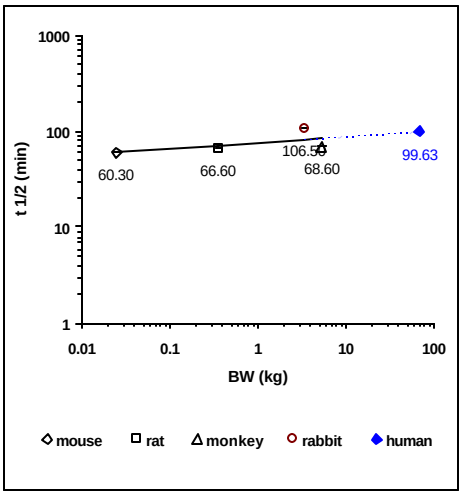

Estimated Human t½=	**99.63**	**minutes**
t½=a*BWb, a=	**75.77**	
b=	**0.06**	
R2=	**0.39**	

Figure 4.6 Allometric scaling of terminal half-life (t½) for RP845-Tc-99m.

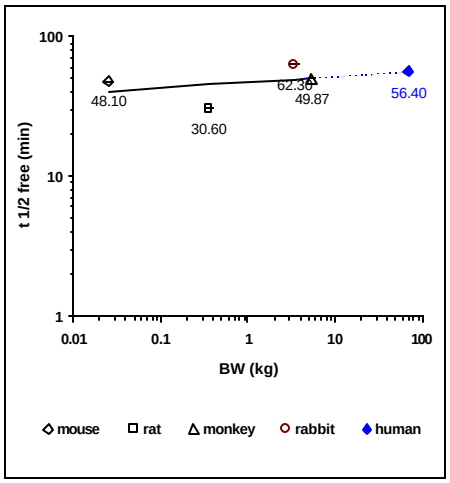

Estimated Human T1/2=	**70.6**	**min**			
T1/2 free=a*BWb, a=	**47.14**				
b=	**0.04**				
R2=	**0.12**				
	Mouse	**Rat**	**Monkey**	**Rabbit**	**Human**
Fraction Unbound (fu)	**0.797**	**0.459**	**0.727**	**0.585**	**0.80**

Figure 4.7 Allometric scaling of terminal half-life (t½) for RP845-Tc-99m corrected for Plasma Protein Binding

Vd_{SS} of RP845 for each animal model was plotted through allometric scaling pre (Figure 4.8) and post (Figure 4.9) correction for plasma protein binding. Vd_{SS} decreased slightly following protein binding correction while the line fit correlation was excellent in both cases.

Overall, predicted pharmacokinetic parameters in human following correction for protein binding were 7.6 mL/min/kg, 70.6 minutes and 0.87 L/kg, for CL, t½ and Vdss respectively.

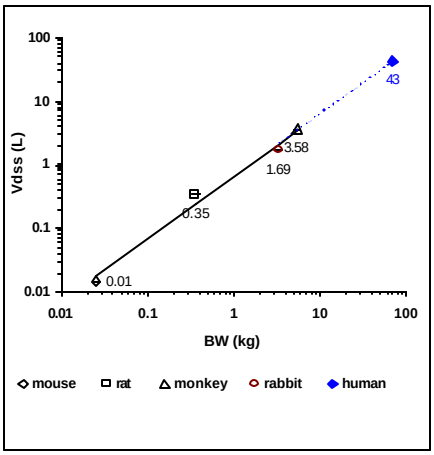

Estimated Human Vdss=	**0.61**	**L/kg**
Vdss=a*BWb, a=	**0.65**	
b=	**0.99**	
R2=	**0.99**	

Figure 4.8 Allometric scaling of Volume of distribution (Vd_{SS}) for RP845-Tc-99m.

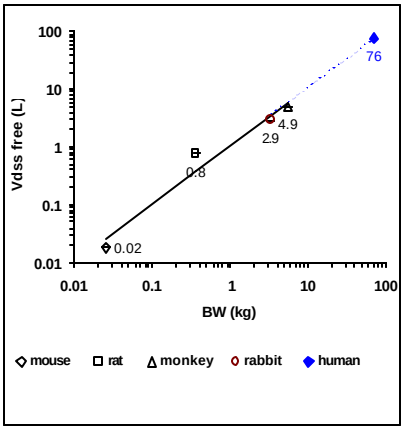

Estimated Human Vdss=	**0.87**	**L/kg**			
Vdss free=a*BWb, a=	**1.05**				
b=	**1.01**				
R2=	**0.97**				
	Mouse	**Rat**	**Monkey**	**Rabbit**	**Human**
Fraction Unbound (fu)	**0.797**	**0.459**	**0.727**	**0.585**	**0.8**

Figure 4.9 Allometric scaling of Volume of distribution (Vd_{SS}) for RP845-Tc-99m corrected for Plasma Protein Binding

4.5 Discussion

Allometric scaling of blood clearance and half-life for predicting non-human primate values improved significantly following correction of protein binding. The line correlation pre and post protein binding correction remained unchanged, however the variation in protein binding between species was enough to improve the accuracy of the predicted pharmacokinetic values once allometric scaling was adjusted. Blood clearance improved from 40% to 12% accuracy, which is significant, as clearance is important when calculating administered dose and compound exposure in the blood. Vd_{SS} accuracy did not improve when corrected for protein binding, however was still 38% accurate. Line fit was > 0.97 pre and post correction for Vd_{SS}. It is also important to recognize that data from only one non-human primate study was used and may have impacted the predictive accuracy for estimating primate data from the three pre-clinical models and also for predicting human results. Adding the one primate study into the analysis of predicting the human pharmacokinetics and ultimately the dose, however should have less impact on variability as the other models help define the extrapolated line estimate. It is also interesting to note in this case that the predicted human pharmacokinetic parameters were very close the non-human primate observed values, which was not always the case in the programs reviewed in chapter three.

Blood clearance in all the models except mouse was faster than the glomerular filtration rate (GFR) of each species, which indicates either kidney secretion or a clearance route other than the kidney is occurring. In the case of the non-human primate,

it is clear from the scintigraphic image that clearance is somewhat hepatobiliary. This same pattern of hepatobiliary elimination may be expected in the human since the predicted blood clearance rate is approximately three times faster than the GFR, which is similar to the non-human primate.

Based on the qualitative image of plaque in the rabbit abdominal aorta (Figure 4.2), a 0.36 mCi*min/ml AUC blood exposure (Table 4.3) was sufficient to visualize the plaque. Assuming the same blood exposure is needed in the human to provide a similar qualitative image of plaque, a dose of 191 mCi/70kg subject would be required. This is calculated by multiplying the predicted blood clearance in human (7.6 mL/min/kg) by the AUC (0.36 mCi*min/ml), which gives a dose of 2.7 mCi/kg. A typical maximum dose for a technetium-99m imaging agent is 0.36mCi/kg. A high dose of 2.7 mCi/kg would potentially result in radiation toxicity to the kidneys or urinary bladder since this compound is excreted renally. Even if the same exposure as achieved in the rabbit was achieved in the human, it is unclear if the plaque could be visualized quantitatively using technetium-99m and a scintillation gamma camera. This concern is based on the resolution and sensitivity of scintigraphic imaging with RP845 Tc-99m, since in previous studies it was insufficient to quantitatively assess plaque burden in the animal models. An increase in plaque uptake or more sensitive imaging capabilities may be necessary for RP845-Tc-99m imaging of atherosclerotic plaque.

Based on the maximum human dose and blood clearance calculated through allometric scaling corrected for protein binding, RP845 would be ineffective as a plaque-imaging agent. Using the predicted pharmacokinetic information provides input into structure-activity relationship (SAR), suggesting modifications that would help change the disposition of the compound. For example, modifying the chemical composition of the compound to decrease blood clearance may enhance uptake at the target. This chapter presents a good example of how using allometric scaling corrected for plasma protein binding to predict blood clearance of the compound in human helped evaluate the compounds targeting potential and success of imaging atherosclerotic plaque.

5. CHAPTER 5

Prediction of “First Dose in Human” for a Myocardial Perfusion Stress Agent Based on Pharmacokinetics in Pre-Clinical Animal Models

5.1 Summary

DPC-A78445-00 is being developed as an alternative to exercise for increasing blood flow in myocardial perfusion imaging for the evaluation of coronary artery disease. DPC-A78445-00 is a C2 and 5' substituted adenosine analog with selective agonist activity for the Adenosine 2a receptor. Stimulation of this receptor mimics exercise stress by directly inducing coronary vasodilation. *In vitro* and *in vivo* pre-clinical studies, including: blood stability, blood clearance, metabolic profiling, mass balance, plasma protein binding and primary hepatocyte assays were conducted in mice, rats, dogs and human models/biological matrices to understand the biological properties of DPC-A78445-00 in each model for use in scaling dose to human. In addition, dog cardiovascular studies were conducted to examine the relationship between pharmacokinetic and pharmacodynamic parameters to understand the pharmacokinetics at the dose level required for appropriate coronary vasodilation. Results indicated DPC-A78445-00 was rapidly metabolized to the carboxylic acid by rodent blood *in vitro* ($t_{1/2} < 30$ seconds) however, longer stability was observed in dog ($t_{1/2}$ 41 minutes) and

human blood (t½ 54 minutes). These findings were confirmed *in vivo*, where plasma levels of DPC-A78445-00 were virtually undetectable immediately after administration in mice and rats, whereas, high levels of the carboxylic acid metabolite were predominant. In contrast, DPC-A78445-00 blood exposure, expressed as area under the blood concentration-time curve (AUC) and blood clearance (CL), in the dog following a 1ug/kg dose were 34.1 ± 10.6 ng*min/mL and 31.6 ± 9.8 mL/min/kg, respectively. *In vitro* primary hepatocyte assays indicated a similar rate of hydrolysis of the DPC-A78445-01 ester to the carboxylic acid derivative in dog and human. Mass Balance recovery was greater than 90% as the carboxylic acid in rats and dogs with the major excretory route for both species being hepatic. Plasma protein binding of DPC-A78445-00 was at a similar, moderate level in rat, dog and human plasma (80-93%). These findings suggest the rat and mouse metabolize DPC-A78445-00 more rapidly than the human and are, therefore, unlikely to be appropriate predictors. In contrast, blood, hepatocyte, and plasma protein binding for DPC A78445-00 was similar in the human and dog and suggesting this species may be an appropriate predictor for the human. This finding was confirmed in a Phase I Human clinical trial that showed the AUC (23.1 ± 3.7 ng*min/mL) and clearance (44.1 ± 6.4 mL/min/kg) were similar in man to that found in the dog.

In conclusion, a thorough *in vitro* and *in vivo* pharmacokinetic assessment of each animal model including blood stability, hepatocyte assays, plasma protein binding and blood pharmacokinetic analysis was necessary to select the appropriate species for scaling to humans. Dog was the only model similar to human with respect to disposition

of DPC-A78445-00 and predicted human pharmcokinetic parameters (Cl, AUC) within 32% of observed values based on body weight.

5.2 Introduction

Radionuclide myocardial perfusion imaging (MPI) is a widely used noninvasive method for the evaluation of myocardial function or disease. MPI is typically done while the heart is resting and under stress to create and detect any flow abnormalities. Exercise stress is the preferred stress modality, however a significant number of patients are unable to reach sufficient exercise levels to cause meaningful coronary vasodilation because of physical conditions. Pharmacological stress agents can be divided into two categories, coronary vasodilating agents (e.g. Dipyridamole and adenosine) and catecholamines (e.g. Dobutamine), depending on their mechanism of action. Vasodilators work directly on the coronary arteries to increase blood flow and catecholamines are positive inotropic and chronotropic agents that increase cardiac workload and potentially cause myocardial ischemia (Hendel *et al*., 2003). Pharmacologic stress using adenosine or dipyridamole is increasingly being employed as an alternative to exercise stress with myocardial perfusion imaging in patients suspected of having coronary artery disease. Although the safety of these vasodilators has been well established, side effects occur frequently and sometimes result in a suboptimal stress test or premature termination of the study (Ranhosky *et al*., 1990; Cerqueira *et al*., 1994). Whereas the desired coronary vasodilatation during adenosine or dipyridamole infusion results from stimulation of the A_{2A} receptor subtype, the undesired side effects are due to stimulation of the other three adenosine-receptor subtypes. A selective adenosine 2a receptor (A2a), therefore, has the potential to produce the required coronary vasodilation without the high incidence of unwanted side effects.

DPC A78445-00 was identified from a series of substituted adenosine analogs as having high selectivity for the A2a receptor and sufficient duration of coronary vasodilation following bolus administration in dogs to allow myocardial perfusion imaging to be performed (Glover *et al*., 2001). DPC-A78445-00 is being developed as a myocardial stress agent as an alternative to exercise in myocardial perfusion imaging for the evaluation of coronary artery disease.

The FDA requires that the "first in human" dose be based on pre-clinical animal model efficacy and safety testing to ensure a safe entry into Phase I clinical trials. Interspecies scaling of pharmacokinetic parameters in the appropriate species is therefore important for predicting drug doses in human clinical trials. The presence of a methyl ester in the structure of DPC-A78445-00 (Figure 5.1) makes this agent potentially susceptible to esterase activity and hydrolysis to the carboxylic acid, which may vary between species. It was therefore important to ensure that the fate of DPC-A78445-00 in the species used in pharmacological models and toxicity studies predict for the human. The stability of DPC-A78445-00 was examined in rat, mouse and dog blood and compared with human blood. It was also necessary to assess the extent of binding to plasma proteins, which will affect free drug availability and altar clearance from the blood.

5.3 Materials and Methods

5.3.1 Chemistry

The structures of DPC-A78445-00 and JR3119 (Internal Standard) are shown in Figure 5.1 and Figure 5.2, respectively. The internal standard is used to correct for losses of the DPC-A78445-00 and the Carboxylic Acid Metabolite during sample handling.

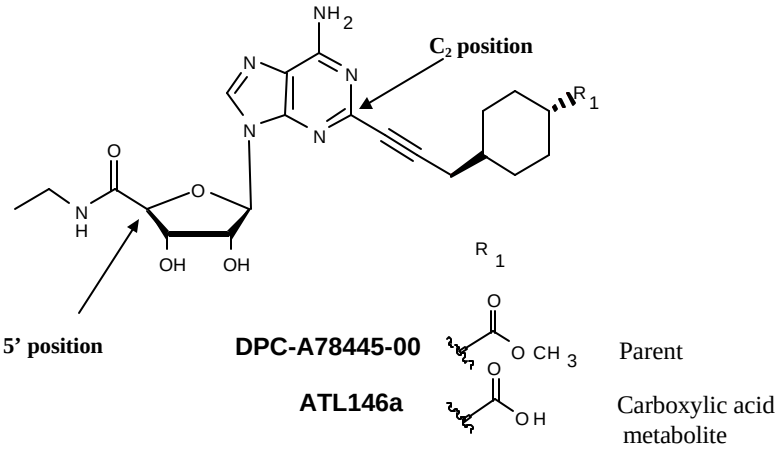

Figure 5.1 Structure of DPC-A78445-00 and the Carboxylic Acid Metabolite (ATL 146a)

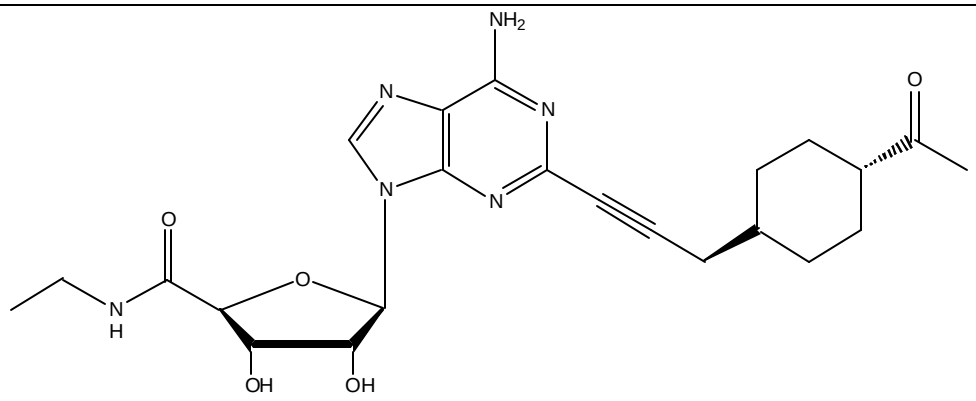

JR3119

$C_{23}H_{30}N_6O_5$
Mol. Wt.: 470.52

Figure 5.2 Structure of JR3119 (Internal Standard)

5.3.2 *In vitro* Blood stability

5.3.2.1 Sample Incubation

DPC-A78445-00 was incubated with fresh heparinized Sprague-Dawley rat, mongrel dog, human (50 nM incubation concentration), and FVB mouse (35 nM incubation concentration) blood at 37°C. Aliquots (1 mL) were taken from rat and mouse blood incubations at 0.5, 1, 2, 5, 15, 30, and 60 minutes and from the dog and human samples at 1, 5, 10, 15, 30, and 60 minutes post-incubation (n=1/timepoint). Blood was transferred directly into 2 mL of acetonitrile containing 70 ng/mL JR3119 (Internal Standard) and assayed immediately for DPC-A78445-00 and the carboxylic acid

metabolite (ATL 146a). An aliquot of control blood was prepared for each species to assess background interference. DPC-A78445-00 was incubated in saline over 2 h to assess non-matrix stability.

5.3.2.2 Sample Extraction

Samples were vortexed for 30 seconds and centrifuged at 2000 x g for 15 minutes. The supernatant was transferred to a fresh tube and centrifuged again to ensure removal of precipitated protein. The supernatant was transferred to a fresh tube where acetonitrile was evaporated under a stream of nitrogen in a heating block at 37°C. Samples were reconstituted to a 1 mL volume with 9% acetonitrile / 0.1% formic acid.

5.3.2.3 DPC-A78445-00 Analysis

Extracted samples and standards (100 µL) were analyzed on a validated mass spectrometry method (Gorman *et al*., 2003) using a Hewlett Packard 1100 multisolvent HPLC delivery system (Hewlett Packard, Burlington, Massachusetts) and an API 3000 MS/MS spectrophotometer (Applied Biosystems, Foster City, California). The analytical column was a Zorbax SB-CN (3.5 µ particle, 4.6 x 150 mm) maintained at a column temperature of 50°C and 1.0 mL flow rate. Mobile phase A was 0.1% formic acid (CH_2O_2), and mobile phase B was 0.1% CH_2O_2 containing 90% acetonitrile. A linear gradient from 10% to 60% mobile phase B over 22 minutes was used for the elution of DPC-A78445-00 and its metabolite. A six minute post-time of 10% mobile phase B was used to equilibrate the column. LC/MS/MS analysis was done in the

electrospray positive ion, MRM scan mode for detection of DPC-A78445-00 (487.0/314.0 amu), JR3119 and ATL 146a (473.0/300.0 amu) m/z. Nitrogen was used as curtain, nebulizing and collision gas with settings of 12, 2 and 10, respectively. Spray voltage was set at 5500 volts and temperature at 450°C. The retention times for ATL 146a, JR3119 and DPC-A78445-00 were 10.0, 11.3 and 12.3 minutes, respectively. A representative chromatogram is shown in Figure 5.3 illustrating resolution of peaks and column retention times. Standard curves for DPC-A78445-00 (0.119 - 91.6 ng/mL) and ATL 146a (0.125 - 94.6 ng/mL) were prepared in 9% acetonitrile/0.1% formic acid. JR3119 was also prepared in the same diluent at 70 ng/mL. Standard curves and internal standard recovery were used for the quantitation of DPC-A78445-00 and ATL 146a in samples. Analyte quantitation was determined using sample volume, peak area of analytes and applying a correction factor based on internal standard recovery.

5.3.2.4 Data Analysis

Sample concentrations of DPC-A78445-00 and ATL 146a were determined by comparison of internal standard (JR3119) adjusted peak area to standard curves for DPC-A78445-00 and the carboxylic acid metabolite (ATL 146a). The percent conversion to the acid metabolite was calculated by dividing the total acid metabolite (ng/mL) by the total acid metabolite and ester (ng/mL) quantitated in the sample. Total DPC-A78445-00 added to samples was recovered as either the ester or acid. Half-life

estimates were made by calculating the time for parent compound to decrease to 50% of initial concentration.

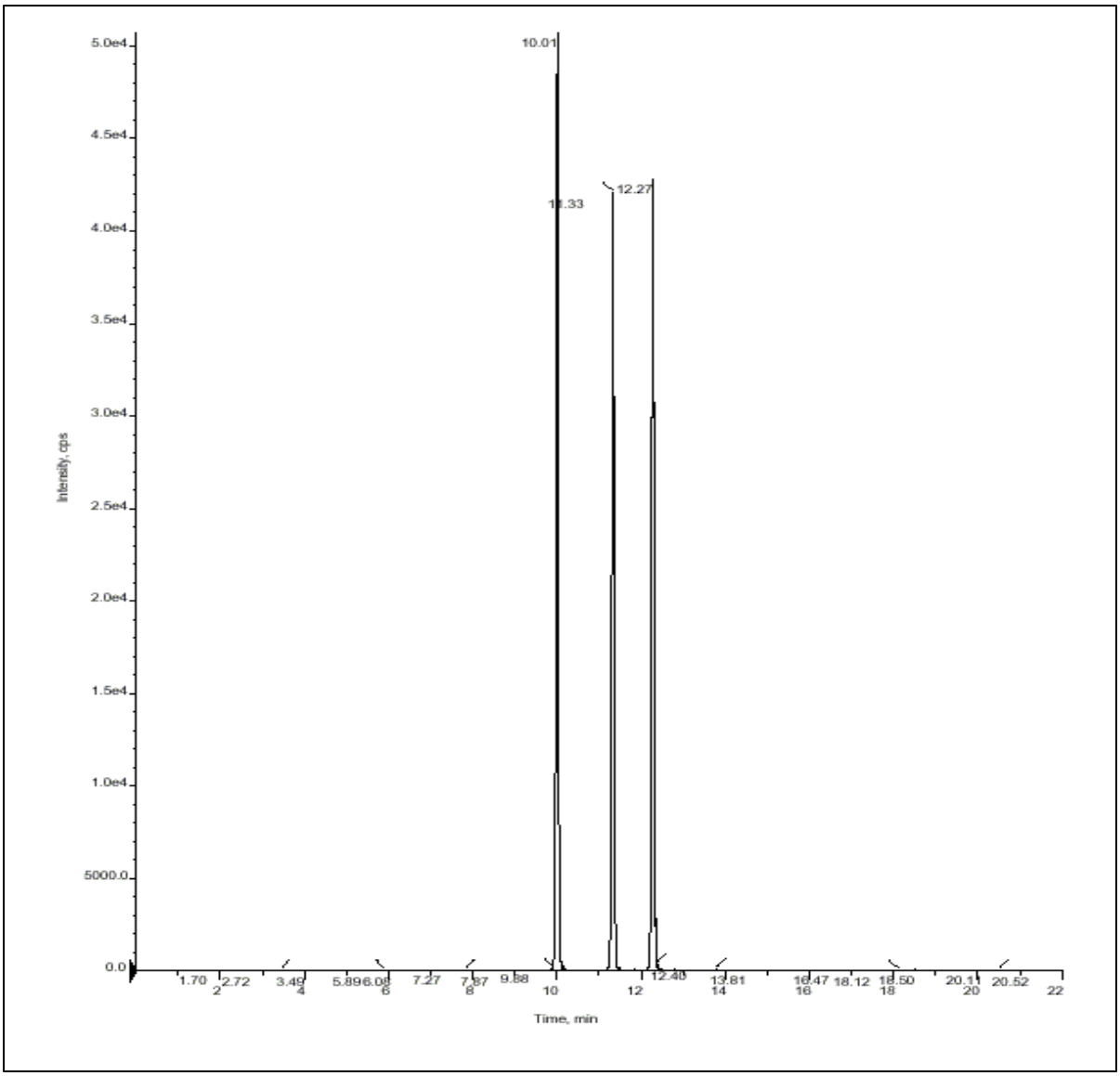

Figure 5.3 Representative LC/MS/MS Chromatogram Illustrating Peak Resolution and Column Retention Times of ATL 146a (RT=10.01), JR3119 (RT=11.33) and DPC-A78445-00 (RT=12.27)

5.3.3 *In vitro* Hepatocyte Metabolism

5.3.3.1 Buffer Preparation

Krebs-Henseleit Buffer (KHB) with 2000 mg/L glucose was purchased from Sigma (St Louis, Missouri) and supplemented with 0.373 g/L of calcium chloride and 2.1 g/L sodium bicarbonate. KHB was adjusted to pH 7.4 (using 1N hydrochloric acid or 1N sodium hydroxide) and sterilized by vacuum filtration using a polyethersulfone (PES) membrane with a porosity of 0.22 μ.

5.3.3.2 Hepatocyte Preparation

Cryopreserved hepatocytes were purchased from *In vitro* Technologies, Inc. (Baltimore, Maryland) and stored at -150°C prior to use. Three lots of human hepatocytes (#104, #129 and #CEK) from male and female donors ranging in age from 53 to 63 with varying medical history and one lot of hepatocytes each for dog (Male Beagle, Lot #VWG) and rat (Male Sprague-Dawley, Lot #REM) were used. On the day of the study, hepatocytes were placed on ice for five minutes to release any liquid N_2 then placed into a 37°C water bath for 75-90 seconds to thaw. The hepatocytes were transferred into pre-warmed KHB and centrifuged for five minutes at 50 x *g*. The supernatant was discarded and the hepatocytes were resuspended in KHB at a concentration of $1x10^6$ cells/mL.

5.3.3.3 Hepatocyte Incubation

Hepatocytes ($1x10^6$ cells/mL) were incubated for up to 2 h at 37°C/5% CO_2 with DPC-A78445-00 diluted in 0.9% saline. Final incubation concentration of DPC-A78445-00 was 50 nM. Rat hepatocytes were sampled at five and 15 minutes post-incubation, dog hepatocytes at 5, 15 and 120 min post-incubation, and human hepatocytes at 1, 5, 15, 30, and 120 min post-incubation. Samples (1 mL) were transferred directly into acetonitrile (2 mL) and internal standard (JR3119, a methyl ketone) was added. Samples were vortexed for 30 seconds, centrifuged at 2000 x *g* for 15 minutes, supernatant decanted and centrifuged again to ensure removal of precipitated protein. The supernatant was transferred to a new tube and dried under a stream of nitrogen in a heating block at 37°C to remove acetonitrile. Extracts were re-constituted in 9% acetonitrile/0.1% formic acid and assayed by LC/MS/MS (section 1.3.2.3). Hepatocytes were incubated alone as controls in all studies for the determination of matrix interference.

5.3.4 Data Analysis

Sample concentrations of DPC-A78445-00 and ATL 146a were determined by comparison of internal standard (JR 3119) adjusted peak area to standard curves for DPC-A78445-00 and the carboxylic acid metabolite (ATL 146a). The percent conversion to the acid metabolite was calculated by dividing the total acid metabolite (ng/mL) by the total acid metabolite and ester (ng/mL) quantitated in the sample.

5.3.5 Pharmacokinetics

5.3.5.1 Animal Dosing

The Institutional Animal Care and Use Committee (IACUC) reviewed protocol procedures and approved all experiments conducted with animals.

5.3.5.1.1 DPC-A78445-00 Clinical Formulation Test Article

Vials containing DPC-A78445-00 (BMS50685-8B; 25.0 µg/mL) in 8.8 mM sodium citrate and 20 mg/mL sucrose buffer were prepared and stored as a frozen solution. Vials without DPC-A78445-00 were also used as a formulation control diluent. All vials were thawed at 22°C and appropriate volumes drawn for injection.

5.3.5.1.2 DPC-A78445-00 Safety Formulation Test Article

Vials containing DPC-A78445-00 (BMS50685-8B, 200 µg/mL) were prepared in 2% DMSO/0.9% sodium chloride for injection. Vials without DPC-A78445-00 were also used as a formulation control diluent. Vials were brought to room temperature and appropriate volumes drawn for injection.

5.3.5.1.3 Rat

Female (~250 g) and male (~340 g) Sprague-Dawley rats were obtained from Charles River Laboratories (Wilmington, Massachusetts). After a 72 h-acclimation period, DPC-A78445-00 clinical formulation was administered via the tail vein as a 150 μg/kg bolus dose in a volume of 6.5 mL/kg.

5.3.5.1.4 Dog

Female dogs (~14 kg) were acclimated in metabolism cages for 24 h prior to the start of the study. After the acclimation period, DPC-A78445-00 safety formulation was administered via the cephalic vein as a 150 μg/kg bolus dose in a volume of 0.75 mL/kg.

Pharmacokinetic and pharmacodynamic parameters were also examined in anesthetized, open-chest dogs. Each dog received four intravenous doses (non-cumulative) of DPC-A78445-00: 0.25, 0.5, 1.0, and 2.0 μg/kg, all in a volume of 2.0 mL. Pharmacokinetic (PK) analysis included C_{max}, area under the (time-plasma concentration) curve (AUC), clearance (CL) and terminal (β-phase) half-life ($t_{1/2}$). Hemodynamic responses, expressed as percent change from baseline values, for each dose level included heart rate, arterial blood pressure, left ventricular dP/dt, and coronary blood flow. Coronary blood flow was measured by fixing a Doppler flow probe to the left anterior descending coronary artery. Similar studies were also performed using the carboxylic acid metabolite of DPC-A78445-00 (ATL 146a) to determine its potential role

in hemodynamic responses. Doses of 0.5, 2.0, 5.0, and 30.0 μg/kg of ATL 146a were evaluated.

5.3.5.1.5 Mouse

Female FVB mice carrying the c-neu Oncogene (~25 g) from our in-house colony were dosed intravenously with the DPC-A78445-00 clinical formulation via the tail vein as a 150 μg/kg bolus dose in a volume of 6.5 mL/kg.

5.3.5.2 Sample Collection

5.3.5.2.1 Blood

Blood samples were collected into heparin treated syringes via terminal heart puncture from individual rats and mice (n=1/time-point) at 1, 3, 5, 7, 10, 15, and 30 minutes post-injection and from the cephalic vein (opposite injection site) of the dog (n=8 time-points/dog, n=3) at 1, 3, 5, 7, 10, 15, 30, and 60 minutes post-injection. Following collection, blood (1 mL) was rapidly added to acetonitrile (2 mL) to denature any esterase and precipitate proteins.

5.3.5.2.2 Urine and Feces

Animals (rats and dogs) were housed in metabolic cages, and samples remained at room temperature (22°C) during the collection period. Urine and feces were collected at intervals of 0-24, 24-48 and 48-72 h post-injection for both rats and dogs. Cage washes were performed with 50% ethanol at the end of each collection interval for the dogs and

at the end of the study for rats. Cage wash recovery of DPC-A78445-00 was added to urine recovery for the respective time interval. All collection tubes were weighed pre- and post-sample collection for use in recovery calculations.

5.3.6 Sample Preparation

Internal Standard (JR3119, a methyl ketone) was added to acetonitrile precipitated blood and standards to correct for loss of compound during sample preparation. Samples were vortexed for 30 seconds and centrifuged at 2000 x g for 15 minutes. The supernatant was transferred to a polystyrene tube and centrifuged again to ensure removal of precipitated protein. Supernatant was collected and placed under a stream of nitrogen in a heating block at 37°C to evaporate the acetonitrile. All blood volumes were determined prior to sample preparation and adjusted to original volume for analyte quantitation. Internal standard was used to correct for loss of compound during sample preparation. Urine and feces samples were extracted immediately following collection intervals. DPC-A78445-00 was extracted from urine following the same procedure used for blood. Acetonitrile (100-800 mL) was added to fecal collections depending on the collection interval and the amount of fecal sample. The first two collection intervals received more acetonitrile to extract/dilute higher expected concentrations.

5.3.7 Data Analysis

LC/MS/MS analysis was conducted on all samples (section 1.3.2.3). Non-compartmental blood pharmacokinetic analysis was performed using WinNonlin™

Professional (Pharsight Corporation, Mountain View, California) software. Volume of distribution at steady state (Vdss), Clearance of drug from the plasma (CL) and Elimination half-life (t½) were calculated.

5.4 *In vitro* Plasma Protein Binding

5.4.1 Protein Binding Method

An *in vitro* ultrafiltration method for measurement of binding of drugs to plasma protein was used in this study. Centrifree® ultrafiltration devices (Amicon, Beverly, Massachusetts) use a molecular weight cutoff of 30,000 daltons to separate bound from free drug.

5.4.2 Sample Preparation

Sprague-Dawley rat and mongrel dog plasma was obtained in house and human plasma was purchased through a commercial vendor (Biological Specialty Corporation, Colmar, Pennsylvania). ^{14}C-DPC-A78445-00 was added to plasma, vortexed and incubated at 37°C for 15 minutes on a rocker platform. ^{14}C-DPC-A78445-00 was also prepared in saline or deproteinized plasma to determine non-specific binding.

5.4.3 Sample Analysis

Plasma, saline or deproteinized plasma (0.025 mL) aliquots (n=4) were transferred to separate vials for pre-filtration counting using a Tri-carb® 2500TR liquid scintillation counter (Perkin Elmer, Gaithersburg, Maryland). A 0.3 mL aliquot of plasma, saline or deproteinized plasma was transferred to a Centrifree® micropartition cartridge (n=4) and centrifuged at 2500 xg for 15 minutes at room temperature. After centrifugation, 0.025 mL aliquots (n=4) of filtrate were transferred to vials for liquid scintillation counting. All samples were counted in 7 mL vials containing 5 mL of Ultima Gold scintillation fluid (Perkin Elmer, Gaithersburg, Maryland).

5.4.4 Data Analysis

The percent of DPC-A78445-00 bound to plasma proteins was calculated using the following equation:

$$\% \text{ Bound} = \frac{\text{DPC-A78445-00 Total} - \text{DPC-A78445-00 Unbound (filtrate)}}{\text{DPC-A78445-00 Total}} \times 100$$

Where:

DPC-A78445-00 Total = Radioactivity (dpm) in 0.025 mL of sample before ultrafiltration.

DPC-A78445-00 Unbound = Radioactivity (dpm) in 0.025 mL of filtrate.

(Data are reported as the mean ± standard error of the mean [SEM].)

5.5 Results

5.5.1 *In vitro* Blood stability

5.5.2 Rat and Mouse

Incubation of DPC-A78445-00 with FVB mouse and Sprague-Dawley rat blood resulted in almost immediate disappearance of the parent compound and accumulation of the carboxylic acid metabolite. At the first time point (0.5 min), more than 85% of the starting DPC-A78445-00 had been depleted (Figure 5.4) in blood by both the rat and mouse. On the basis of the early time points, the t½ values for DPC-A78445-00 were estimated (Table 5.1). No matrix interference was observed in mouse or rat blood. DPC-A78445-00 incubated in saline over 2 h showed no conversion to the acid metabolite.

5.5.3 Dog and Human

Incubation of DPC-A78445-00 (50 nM) with mongrel dog and human blood resulted in a slow decrease of DPC-A78445-00 (Figure 5.4).

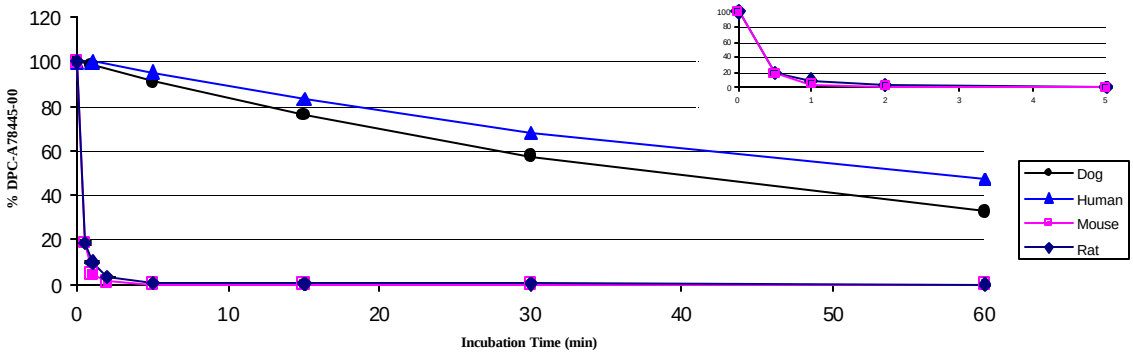

Figure 5.4 Stability of DPC-A78445-00 Over Time in Mouse, Rat, Dog, and Human Blood Following Incubation at 50 nM

The decrease in parent compound was paralleled by an increase in the carboxylic acid metabolite. At the end of the incubation (60 min) the DPC-A78445-00 concentration in dog and human blood respectively was 16.3 nM (32.6% of initial ester concentration) and 23.7 nM (47.4% of initial ester concentration). Based on the DPC-A78445-00 depletion curve, the t½'s for dog and human blood were calculated (Table 5.1). No matrix interference was observed for dog or human blood.

Table 5.1 Half-life of DPC-A78445-00 Incubated in Mouse, Rat, Dog, and Human Whole Blood

Compound	Mouse	Rat	Dog	Human
A78445- $t_{1/2}$	< 0.5 min	< 0.5 min	41.4 min	54.3 min

DPC-A78445-00 was incubated with fresh heparinized blood from the FVB mouse (35 nM), Sprague-Dawley rat (50 nM), mongrel dog (50 nM), and human (50 nM)

DPC-A78445-00 was rapidly ($t_{1/2}$ <0.5 min) converted to the carboxylic acid metabolite in rodent blood. In contrast, the conversion was much slower ($t_{1/2}$ > 40 min) in

dog and human blood. This finding suggests that esterase activity in rat and mouse blood is either lower or absent in dog and human blood. Differences in esterase activity between species are well-established (Minagawa *et al*., 1995). Furthermore, a carboxylesterase has been identified that is released into the blood of rodents that is not present in higher species (Buchwald, 2001). The similar rate of conversion in dog and human blood supports the dog being an appropriate model for vivo assessment of DPC-A78445-00.

5.5.4 *In vitro* Hepatocyte Metabolism

Results indicate DPC-A78445-00 at 50 nM is rapidly metabolized by rat hepatocytes with 97 ± 1.9% and 100 ± 0.4% converted to the acid metabolite (ATL 146a) by five and 15 min, respectively. In human and dog hepatocytes, DPC-A78445-00 conversion to ATL 146a was slightly less rapid with a 97 ± 1.4%and 100 ± 0.1% conversion by 15 and 120 min, respectively, in human, and 73 ± 3.3% and 98 ± 1.6% conversion by 15 and 120 min, respectively, in dog. The percentage of DPC-A78445-00 converted to the acid metabolite at respective time points is shown in Table 5.2. Hepatocyte metabolism in human, dog and rat following incubation of DPC-A78445-00 (50 nM) is depicted in Figure 5.5. Comparison of three different lots of human hepatocytes showed similar conversion to the acid metabolite at 15 minutes (94.8%, 99.5% and 96.5%) and 120 minutes (99.7%, 100% and 99.6%). The total amount of

DPC-A78445-00 added to incubations was accounted for as DPC-A78445-00 or acid metabolite in samples analyzed.

Table 5.2 Hepatocyte Metabolism of DPC-A78445-00 Incubated at 50 nM in Rat, Dog and Human Hepatocytes. Percent Converted to the Acid Metabolite (± SEM)

Incubation Time (min)	Human	Dog	Rat
1	31.2	-	-
5	65.6	48.0 ± 3.9	97.0 ± 1.9
10	87.7	-	-
15	94.8, 99.5, 96.5[a]	73.0 ± 3.3	100.0 ± 0.4
30	99.3	-	-
120	99.7, 100, 99.6[a]	98.0 ± 1.6	-

[a]3 separate lots of human hepatocytes
Human 15 and 120 min, Dog 5 min, Rat 5 min: n=3 replicates/same lot
Dog 15 and 120 min, Rat 5 min: n=4 replicates/same lot
Human 1, 5, 10, and 30 min: n=1 replicate/same lot

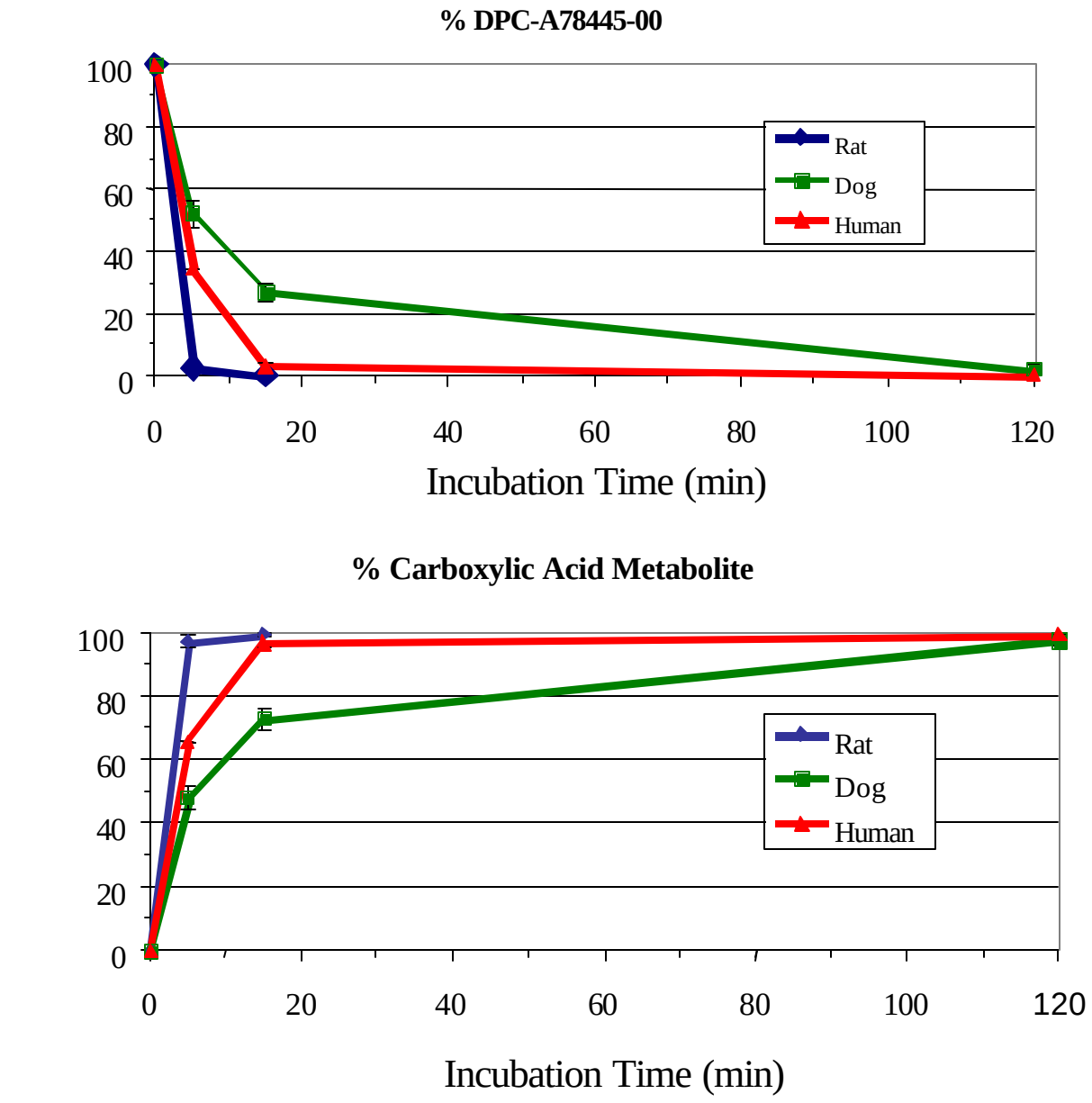

Figure 5.5 Hepatocyte Metabolism of DPC-A78445-00 in Rat, Dog and Human. Loss of Parent Compound and Formation of Metabolite

Rat hepatocytes converted DPC-A78445-00 to the carboxylic acid metabolite almost immediately (97% converted by five minutes). Rapid conversion is also seen with both dog and human hepatocytes. These data are consistent with high levels of esterase activity being present in the liver (Satoh T, *et al*., 1995). The rapid conversion of DPC-A78445-00 by both human and dog hepatocytes supports the dog being appropriate for *in vivo* assessment of DPC-A78445-00. These results indicate that human, dog and rat hepatocytes handle DPC-A78445-00 in a similar manner and result in rapid hydrolysis to the carboxylic acid metabolite. The rapid conversion of DPC-A78445-00 by both human and dog hepatocytes also supports the dog being appropriate for vivo assessment of DPC-A78445-00.

5.5.5 Plasma Protein binding

Plasma protein binding results were similar between species at 50-200 nM with $91.0 \pm 0.1\%$, $85.3 \pm 0.4\%$ and $92.6 \pm 0.2\%$ protein bound for rat, dog and human, respectively. Protein binding for the 500 nM incubation in dog and human plasma was $79.4 \pm 0.4\%$ and $89.8 \pm 0.1\%$, respectively. Non-specific binding at 500 nM in saline and deproteinized human plasma was $22.7 \pm 2.0\%$ and $24.9 \pm 1.4\%$, respectively (Table 5.3). Non-specific binding was similar at 50 nM.

Table 5.3 Percent of ^{14}C-DPC-A78445-00 Bound to Plasma Proteins *In vitro* at 15 Minutes of Incubation in Human, Dog and Rat

	Species					
DPC-A78445-00	**Human**		**Dog**		**Rat**	
Concentration (nM)	**Mean**	**SEM**	**Mean**	**SEM**	**Mean**	**SEM**
50	92.6	0.2	85.3	0.4	[a]91.0	0.1
500	89.8	0.1	79.4	0.4	-	-

[a]Incubation at 200 nM
Values not adjusted for non-specific binding (Saline=22.7 ± 2.0, Deproteinized human plasma=24.9 ± 1.4)
All samples were incubated for 15 minutes.
SEM=Standard Error of the Mean for three replicate filtrates counted three times each.

Protein binding is moderate in plasma from all species tested. The small difference in protein binding between species may be attributed to the different binding properties of the type and quantity of proteins unique to each species. Similar levels of binding were seen in human and dog plasma at either 50 or 500 nM. These data suggest that similar *in vivo* protein binding would be expected between human and dog with the same free drug available to target the A2a receptor. In conclusion, plasma protein binding of DPC-A78445-00 is similar for the rat, dog and human.

5.5.6 Pharmacokinetics

5.5.6.1 Blood Pharmacokinetics

The blood concentration -time profiles following a single I.V. dose of 150 µg/kg DPC-A78445-00 in the mouse, rat and dog are depicted in Figure 5.6 and Figure 5.7. Blood levels of DPC-A78445-00 were low (< 0.1 ng/mL by five minutes) and the carboxylic acid metabolite levels were high in rats (female and male) and mice at early time points. This almost immediate conversion prevented pharmacokinetic parameter analysis for DPC-A78445-00 in the rat or mouse. The carboxylic acid metabolite in the

rat (male and female) and mouse (female) had similar Cmax, terminal half-life and AUC (Table 5.4).

Blood levels of DPC-A78445-00 in the dogs were higher than the carboxylic acid at early time points (one and three minutes) but declined to below metabolite levels after five minutes (Figure 5.7). The Cmax, terminal half-life ($t_{½}$), systemic clearance (CL), area under the curve (AUC_{0-8}), and volume of distribution at steady state (Vd_{ss}) of DPC-A78445-00 in the dog was 746 ng/mL, 9.0 min, 93.9 mL/min/kg, 1561 ng*min/mL, and 0.24 L/kg, respectively (Table 5.5). The carboxylic acid metabolite had a Cmax, terminal half-life and AUC of 55 ng/mL, 19.8 min and 1303 ng*min/mL, respectively (Table 5.4).

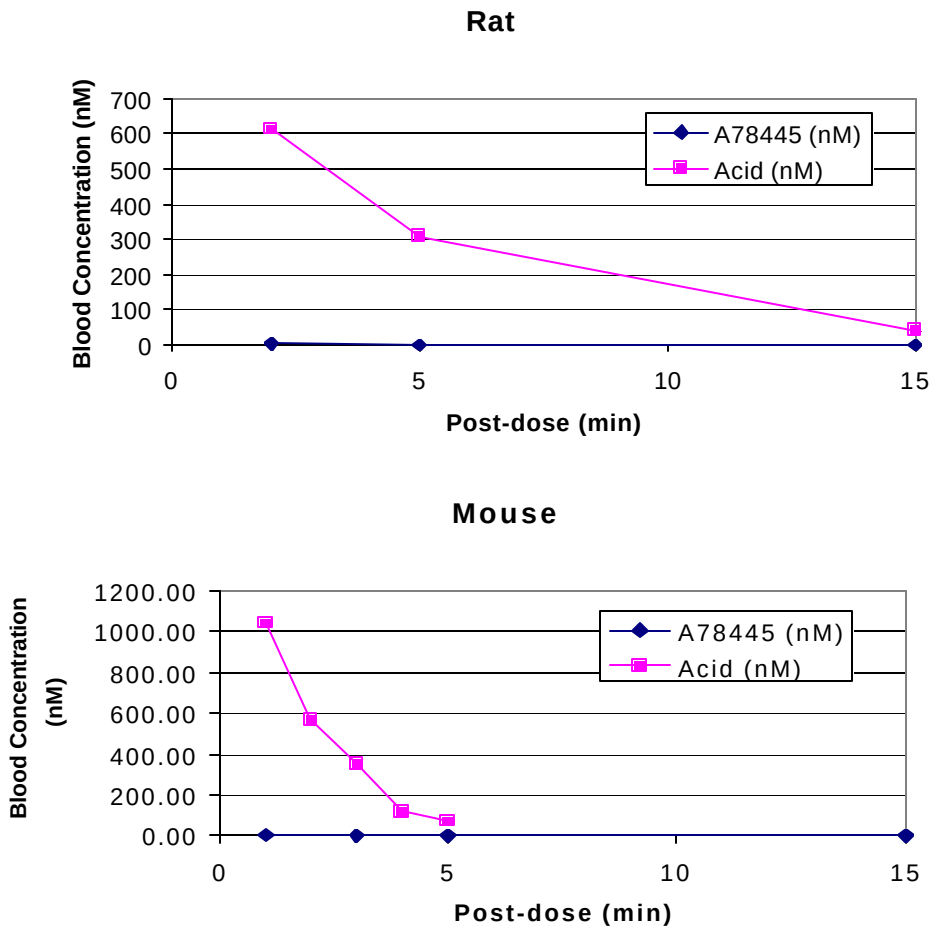

Figure 5.6 Blood Levels of DPC-A78445-00 and the Carboxylic Acid (ATL 146a) Metabolite in the Rat or Mouse Following an I.V. Bolus Dose of 150 µg/kg

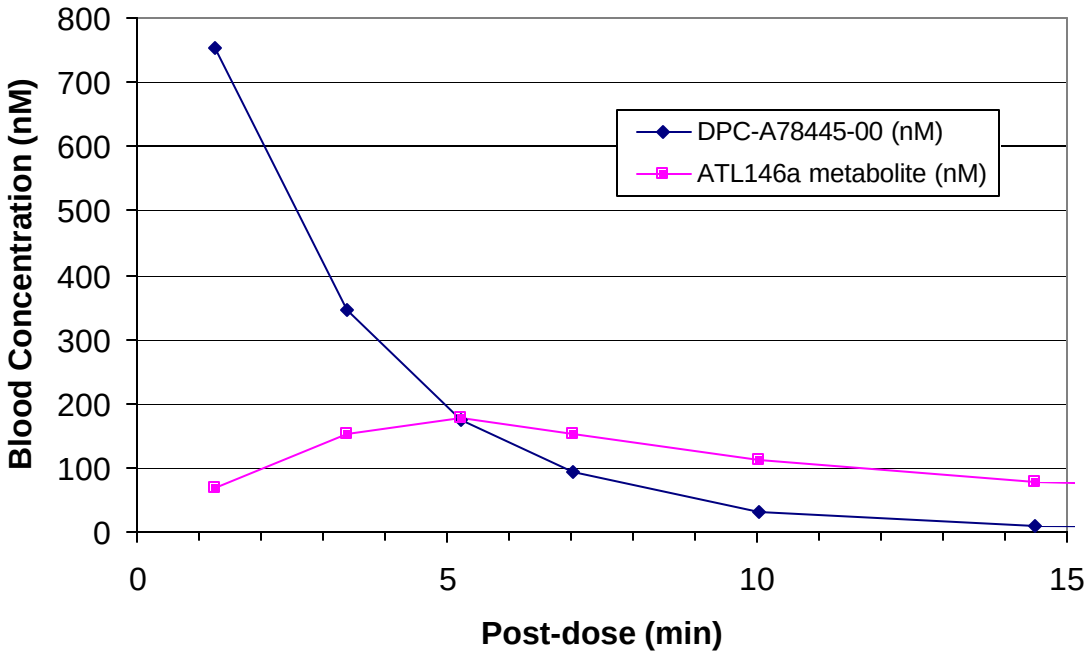

Figure 5.7 Blood Levels of DPC-A78445-00 and the Carboxylic Acid (ATL 146a) Metabolite in Dog Following an I.V. Bolus Dose of 150 µg/kg

Table 5.4 Blood Pharmacokinetics of ATL 146a Carboxylic Metabolite Following an I.V. Dose of 150 μg/kg DPC-A78445-00 in Dogs, Rats and Mice

Species / #Animals	**Cmax (ng/mL)**	**AUC (0-¥) (ng? min/mL)**	**T½ (terminal) (min)**
Dog (female) / n=3	54.7 ± 27.7	1303 ± 595	19.8 ± 2.0
Rat (female) / n=1/Time-point	579	2315	7.5
Rat (male) / n=1/Time-point	386	2039	8.7
Mouse (female) / n=1/Time-point	494	2177	8.1

Mean ± SD

Table 5.5 Blood Pharmacokinetics of DPC-A78445-00 Following an I.V. Dose of 150 μg/kg in Dogs (n=3)

Dose (mg/kg)	**Cmax (ng/m)L**	**AUC (0-¥) (ng? min/mlL**	**T½ (terminal) (min)**	**CL (mL/min/kg)**	**Vdss (L/kg)**
150	746 ± 157	1561 ± 339	9.0 ± 2.0	93.9 ± 22.6	0.24 ± 0.04

Mean ± SD

5.5.7 Dog pharmacokinetics/pharmacodynamics

Measurement of blood levels of DPC-A78445-00 showed a dose-related increase in C_{max} and AUC (Table 5.6). After administration of the target dose of 1.0 μg/kg, clearance averaged 31.6 ± 9.8 mL/min/kg and the terminal half-life was 7.5.± 2.9 minutes. Nearly identical values for these two parameters were observed with the highest dose (2.0 μg/kg), as well. The blood clearance rate of DPC-A78445-00 following I.V administration of the same test article is close to the literature value for hepatic blood flow in the dog (30.9 mL/min/kg) suggesting hepato-biliary clearance (Davies *et al*., 1993). Bolus intravenous administration of DPC-A78445-00 to dogs produced a dose-related increase in both magnitude and duration of coronary blood flow from 0.25 to 2

μg/kg, which correlates well with the pharmacokinetic data (Figure 5.5). Coronary blood flow was measured by fixing a Doppler flow probe to the left anterior descending coronary artery. The dose to produce the required clinical response is 1 μg/kg based on coronary blood flow. This dose was selected based on achieving a sufficient elevation in blood flow over a 6-8 minute duration and acceptable drop in peripheral blood pressure.

The pharmacokinetic parameters for DPC-A78445-00 in the dog indicated a dose of 150 μg/kg produced a very high circulating level that was very rapidly cleared. However, when compared to lower doses, the pharmacokinetic data were not linear. The Cmax and AUC were slightly lower than would have been predicted for the 150 μg/kg dose. In the current study the clearance rate was greater than resting hepatic blood flow in the dog (30.9 mL/min/kg) and the steady state volume of distribution was high. The changes in these parameters at this dose level may be the consequence of DPC-A78445-00 influencing peripheral vasodilation and changing hepatic blood flow (Sakata *et al*, 1999).

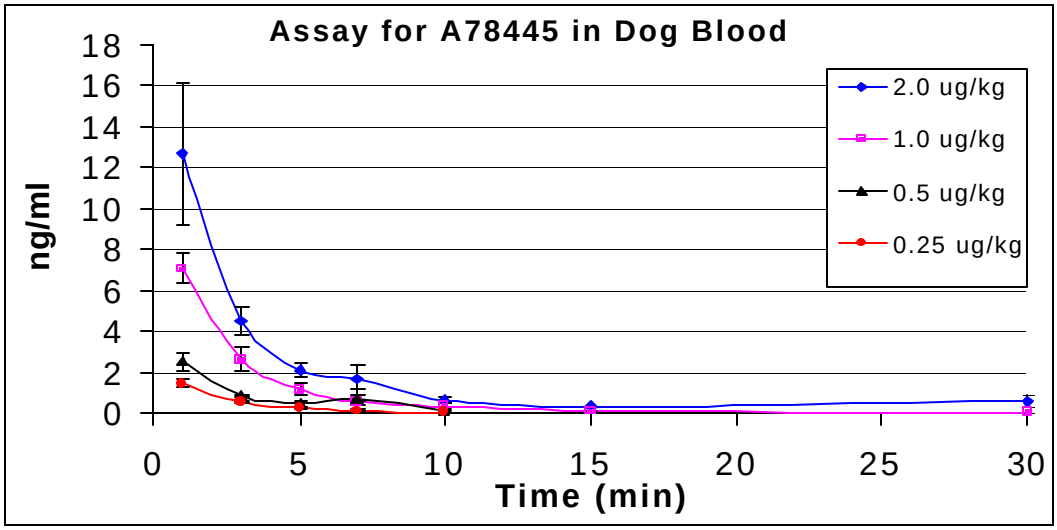

Figure 5.8 DPC-A78445-00 Blood Levels Following I. V. Bolus Administration

5.5.8 PK Analysis of the carboxylic acid metabolite after administration of DPC-A78445-00

Measurement of plasma levels of ATL 146a following the administration of DPC-A78445-00 to anesthetized dogs showed a dose-related increase for both Cmax and AUC (Table 5.7). After administration of the pharmacologically active dose of 1.0 µg/kg of DPC-A78445-00, the C_{max} of ATL 146a was only 0.8 ng/mL - one-fourth the plasma concentration observed when 0.5 µg/kg of the carboxylic acid metabolite itself was administered to a separate group of dogs (Table 5.8). The terminal half-life of the carboxylic acid metabolite averaged 18.3 min, 2.4-fold longer than the half-life observed for DPC-A78445-00.

5.5.9 PK Analysis of the carboxylic acid metabolite (ALT 146a) after administration of this metabolite

Table 5.8 shows the blood pharmacokinetic data from a set of experiments in which the metabolite was administered to anesthetized dogs as an IV bolus at doses ranging from 0.5 to 30 μg/kg. These studies were performed to more completely understand the pharmacodynamic and pharmacokinetic behavior of the carboxylic acid metabolite. Administration of 0.5 μg/kg of ATL 146a produced a C_{max} of 3.3 ng/ml, a value that was approximately twice that observed after administration of 2 μg/kg of DPC-A78445-00 (1.6 ng/mL). The clearance rate of ATL 146a ranged between 20 and 25 mL/min/kg with the four doses evaluated, averaging 22.1 mL/min/kg. This value is approximately 30% slower than the clearance of DPC-A78445-00, consistent with a longer (≅ 2.6-fold) elimination half-life for the carboxylic acid metabolite.

Table 5.6 Blood Pharmacokinetics of DPC-A78445-01 Following I.V. Administration of DPC-A78445-00 in Dogs (n=4)

Dose (mg/kg)	**Cmax (ng/ml)**	AUC **(0-inf) (ng.min/mL)**	$T_{1/2}$ **(terminal) (min)**	**CL (ml/min/kg)**	**Vdss (L/kg)**
0.25	2.6 ± 0.8	7.7 ± 3.2	2.8 ± 0.8	35.8 ± 11.8	0.11 ± 0.04
0.5	4.5 ± 1.6	12.0 ± 3.6	3.9 ± 2.0	45.1 ± 13.2	0.17 ± 0.05
1	12.1 ± 2.4	34.1 ± 10.6	7.5 ± 2.9	31.6 ± 9.8	0.15 ± 0.03
2	29.8 ± 2.2	65.3 ± 15.2	7.3 ± 0.8	31.7 ± 6.3	0.12 ± 0.01

Table 5.7 Pharmacokinetic Parameters of ATL 146a (Acid Metabolite) in Dogs (n=4) Following I.V. Administration of DPC-A78445-00

Dose (mg/kg)	**Cmax (ng/mL)**	**AUC (0-inf) (ng.min/mL)**	**$T_{1/2}$ (terminal) (min)**
0.5	0.6 ± 0.27	11.2 ± 6.7	10.7 ± 2.2
1	0.8 ± 0.26	28.9 ± 12.5	22.8 ± 6.5
2	1.6 ± 0.15	51.2 ± 6.11	22.7 ± 3.6

Table 5.8 Pharmacokinetic Parameters of ATL 146a (acid metabolite) in Dogs (n=6) Following I.V. Administration of ATL 146a

Dose (mg/kg)	**Cmax (ng/mL)**	**AUC (0-inf) (ng.min/mL)**	**$T_{1/2}$ (terminal) (min)**	**CL (ml/min/kg)**	**Vdss (L/kg)**
0.5	3.3 ± 2.2	26.0 ± 11.3	20.3 ± 11.5	21.5 ± 6.8	0.41 ± .02
2	15.2 ± 8.1	104.1 ± 35.9	19.6 ± 6.7	20.8 ± 5.8	0.42 ± 0.19
5	38.0 ± 14.0	257.5 ± 56.2	19.2 ± 3.5	20.2 ± 4.1	0.43 ± 0.11
30	233.7 ± 123.1	1232.6 ± 295.6	14.2 ± 7.6	25.7 ± 7.3	0.43 ± 0.34

Concentration of DPC-A78445-00 in blood correlates with increase in coronary blood flow with increasing doses (Figure 5.5).

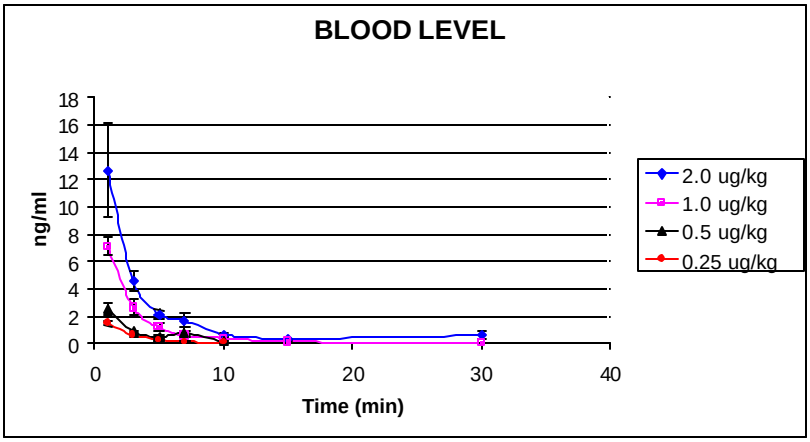

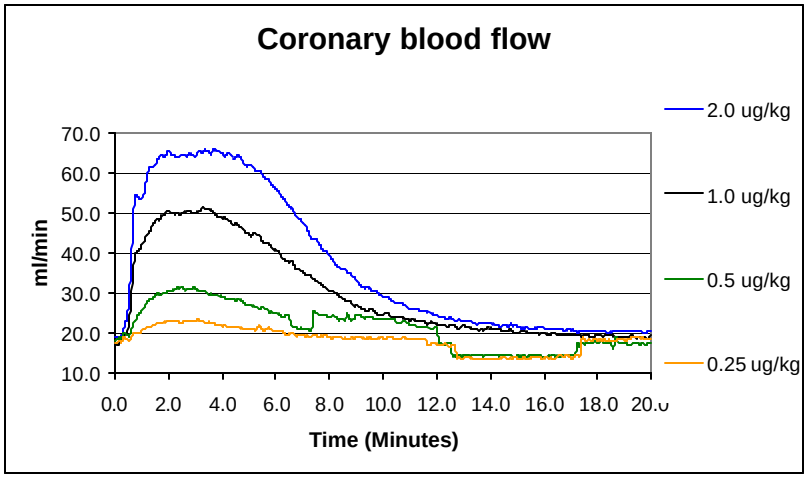

Figure 5.5 DPC-A78445-00 Effect on Coronary Blood Flow and Blood Levels Following I.V. Bolus Administration

5.5.9.1 Mass Balance

Total recovery of DPC-A78445-00 and the carboxylic acid metabolite in mass balance studies in rats was almost complete by 72 h with the majority cleared in the feces for both male and female (Table 5.9). The majority (> 80%) of the dose was excreted as the carboxylic acid metabolite within the first 24 h (Table 5.9). Total recovery of DPC-A78445-00 and the carboxylic acid metabolite in the mass balance studies in dogs was also almost complete by 72 h with the feces being the major route of excretion (Table 5.10). The majority (> 83%) of DPC-A78445-00 was excreted in dogs over the first 48 h as the carboxylic acid metabolite. Results from the study conducted with primary hepatocytes described previously indicated rapid metabolism of DPC-A78445-00 to the carboxylic acid metabolite (ATL 146a), which explains why this metabolite was the only form of DPC-A78445-00 found in fecal excretion. Comparison of male and female rats did not indicate a major difference in mass balance results. The experimental group sizes were very small, therefore statistical comparison was not performed.

Table 5.9 Percent Recovery of an Intravenous Dose of DPC-A78445-00 in Excreta Collected from Female and Male Rats (n=4/sex)

Collection Interval, h	% Urine	SEM (+/-)	% Feces	SEM (+/-)	% Recovery	SEM (+/-)
Female						
0-24	3.7	0.79	79.3	3.35	83.0	3.84
24-48	0.1	0.03	11.1	3.00	11.1	3.01
48-72	0.4	0.15	0.3	0.12	0.7	0.26
Total % Recovery	4.1	0.81	90.6	2.56	94.8	2.34
Male						
0-24	10.1	1.03	79.3	6.66	89.3	5.73
24-48	0.2	0.05	7.3	2.82	7.6	2.82
48-72	0.4	0.06	0.2	0.06	0.6	0.11
Total % Recovery	10.7	1.11	86.7	3.97	97.4	3.06

Table 5.10 Percent Recovery of an Intravenous Dose of DPC-A78445-00 in Excreta Collected from Female Dogs (n=3)

Collection Interval,h	Urine	SEM (+/-)	Feces	SEM (+/-)	% Recovery	SEM (+/-)
0-24	8.2	1.58	21.4	21.38	29.6	21.60
24-48	5.1	4.88	48.7	24.47	53.8	19.67
48-72	3.3	2.76	3.3	2.75	6.6	5.51
Total % Recovery	16.7	3.63	73.3	4.53	90.0	1.04

5.5.9.2 Metabolism

DPC-A78445-00 was almost immediately converted to the carboxylic acid metabolite in the blood of rats and mice. In contrast, blood levels of DPC-A78445-00 in the dogs were higher than the carboxylic acid at early time points (one and three minutes) but declined to below metabolite levels after five minutes. Figure 5.9 and Figure 5.10 show representative LC/MS/MS chromatograms in rat and dog blood, respectively. Both species showed only carboxylic acid metabolite (ALT 146a) and no DPC-A78445-00 in the urine and fecal samples at all collection times. The recovery in mass balance studies indicated the carboxylic acid metabolite could account for > 90% of the administered DPC-A78445-00 dose in both rats and dogs. This indicates the carboxylic acid metabolite is the only major metabolite.

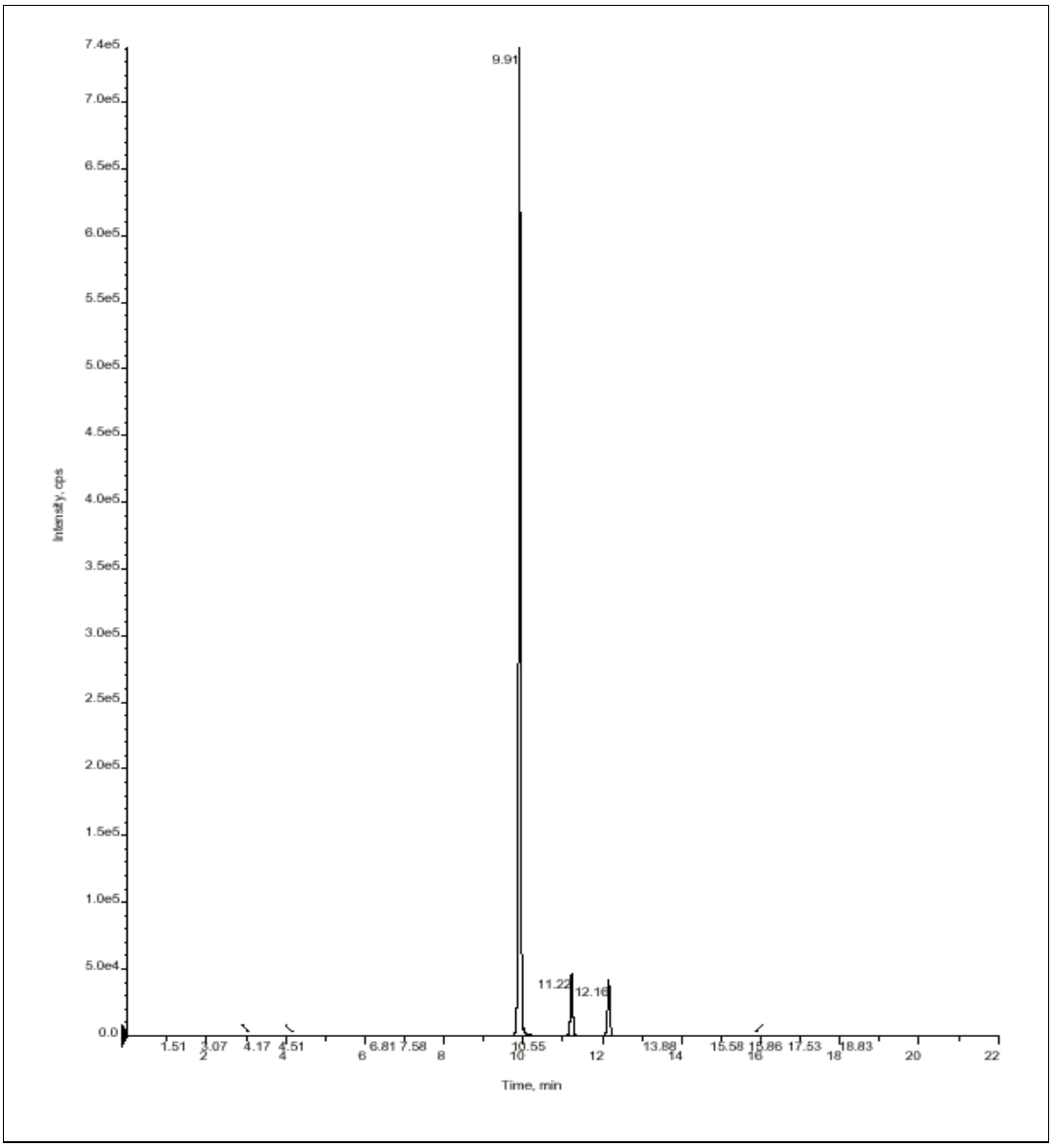

Figure 5.9 Representative LC/MS/MS Chromatogram of DPC-A78445-00 Extracted From Rat Blood 1 min Post-injection (ATL 146a Acid Metabolite=RT 9.9 min, JR3119 Internal Std=RT 11.2 min, DPC-A78445-00=RT 12.1 min)

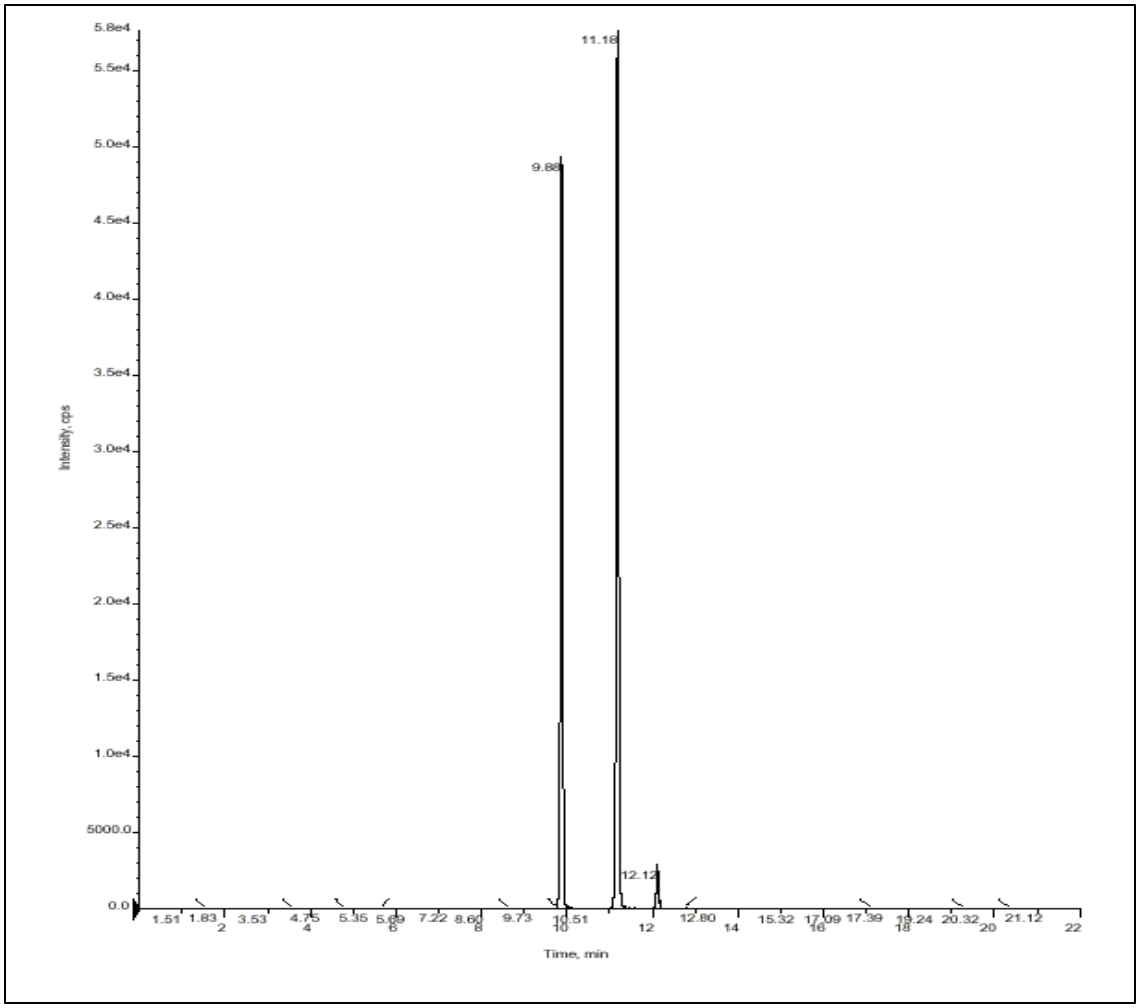

Figure 5.10 Representative LC/MS/MS Chromatogram of DPC-A78445-00 Extracted From Dog Blood 30 min Post-injection (ATL 146a Acid Metabolite=RT 9.8 min, JR3119 Internal Std=RT 11.1 min, DPC-A78445-00=RT 12.1 min)

DPC-A78445-00 was non-detectable in rat and mouse blood samples by five minutes post-dose, which is consistent with hydrolysis occurring in the blood. In contrast, blood samples from the dog indicated high circulating levels of parent compound at early time points with limited levels of the carboxylic acid metabolite (ATL 146a). These findings are consistent with the findings of the current work for stability of DPC-A78445-00 when incubated with

rodent or dog blood *in vitro*. The rapid conversion of DPC-A78445-00 to the carboxylic acid metabolite (ATL 146a) seen in mice and rats compared to slower conversion in dogs may be explained by the higher esterase activity (100-400x) reported for rat whole blood, as compared to dog and human blood (Minagawa *et al*, 1995).

In conclusion, following I.V. administration, DPC-A78445-00 is converted in the blood of rats and mice very rapidly to the carboxylic acid metabolite resulting in minimal systemic exposure to the parent compound. Administration of DPC-A78445-00 to dogs results in high circulating levels of parent compound at early time points. While both DPC-A78445-00 and the carboxylic acid metabolite are rapidly cleared, a slightly longer half-life for the metabolite results in the metabolite levels exceeding the parent compound after five minutes post-dose. Elimination of DPC-A78445-00 in both rats and dogs is predominantly in the feces as the carboxylic acid metabolite.

5.6 Discussion

This chapter emphasizes the importance of understanding the disposition of a compound in each species prior to using it for allometric scaling predictions. The presence of a methyl ester in DPC A78445-00 presented a potential for rapid hydrolysis to the carboxylic acid. The short duration of pharmacological activity in the dog model suggested rapid clearance and made it critical to understand the handling of DPC A78445-00 in the dog and ensure it represented the human. The handling of DPC-A78445-00 was therefore examined in rat and dog blood, whole animal studies of metabolism, pharmacokinetics, elimination and primary hepatocyte metabolism. These results were compared with human blood stability and human hepatocyte metabolism. From these studies, it was recognized the dog and human handle DPC A78445-00 in a similar manner. In contrast, rats hydrolyze DPC-A78445-00 to its carboxylic acid metabolite very rapidly in whole blood. The similar profile of DPC-A78445-00 in dog blood and dog hepatocytes to human blood and human hepatocytes supports the dog being an appropriate testing species. Pharmacokinetic and mass balance studies in the dog indicated hepatic clearance at a rate equivalent to hepatic blood flow. This data indicates that human clearance of DPC-A78445-00 will be hepatic and at a rate approximating human hepatic blood flow.

Based on the pharmacology studies in the dog model, a bolus dose of 1ug/kg DPC A78445-00 was identified as producing a sufficient increase in coronary blood flow to allow stenosis imaging with a perfusion tracer. The selected dose of 1 ug/kg for human clinical trials was the optimal dose that elicited an acceptable increase in heart rate with

fewer adverse events than the commercially available vasodilator, adenosine™ (Hendel *et al*., 2005). The blood exposure, or area under the curve, for a 1ug/kg dose of DPC-a78445-00 in dogs was 34.1± 10.6 ng*min/mL. In contrast, the exposure in human for the same dose was 23.1± 3.7. The large standard deviation in the dog may indicate an overestimate of the difference in results. A comparison of dose at 0.25 ug/kg in the dog to 0.3 ug/kg in human, indicates an AUC of 7.7±3.2 and 6.3±1.8 ng*min/mL, respectively. The percent difference between dog and human at both dose levels is <32%. The prediction of a 1 ug/kg dose for humans, made prior to the start of clinical trials based on body weight using pharmacokinetic data from only the dog, proved to be an extremely accurate prediction. This project emphasizes the need to fully characterize all pre-clinical animal models with respect to pharmacokinetics to ensure using the correct model data for prediction of human dose.

6. CHAPTER 6

6.1 General Conclusions and Future Research

6.1.1 Summary and conclusions

The overall goal of this research was to examine the feasibility of using weight based allometric scaling as a predictive tool to estimate human pharmacokinetic parameters from pre-clinical animal data. Data for three imaging agents and a pharmacological stress agents (Oncology tumor agent (DPC-A80351), Thrombus agent (DMP-444), Infection agent (RP-517) Pharmacological stress agent (DPC-A78445-00)) that entered human clinical trials, and an imaging agent being developed (RP845) were assessed for scaling accuracy. Initially pharmacokinetic data from animal models were used to extrapolate to human though body weight allometric scaling. Subsequently the impact of adjusting for plasma protein binding and the impact of metabolic stability in the different models was examined.

Allometric scaling of animal pharmacokinetic parameters (clearance, half-life and volume of distribution) achieved a prediction of the human pharmacokinetic parameter with an accuracy of 13 to 109% for the three imaging agents with available clinical data. This prediction was further improved by adjusting for plasma protein binding of the drug and achieved an accuracy of 5 to 57% of the clinically observed values. This level of predictivity closely approached the thesis target of achieving a mathematical model that would allow prediction of human dose within 30%. In fact, if clearance was taken as the primary pharmacokinetic value, the weight based allometric scaling with protein binding

adjustment was predictive within 12.5 % based on a retrospective analysis. Recent work by Tang and co-workers (2005), reported predicting human clearance values within 78% with a new method using rat and human data only. They also compared their accuracy with simple allometric scaling (323%) and the rule of exponents (185%). A 12.5% prediction accuracy is excellent considering recently published literature and would provide clinical dose estimates within a much smaller range.

Weight based allometric scaling was further examined for an atherosclerotic plaque targeted radiopharmaceutical imaging agent, RP845-Tc-99m, currently in development. Pharmacokinetic parameters were determined in mouse, rat and rabbit, allometric scaling was used to predict the non-human primate value. Differences between predicted versus observed non-human primate Cl, t½ and $Vd_{SS,}$ were 40%, 52% and 8%, respectively. Correcting for plasma protein binding improved the prediction for Cl and t½ to within 12 and 3 %, respectively. Vdss prediction, however, became less accurate (38% difference). Since blood clearance is the major parameter in predicting human dose, the improvement from 40% to 12% accuracy is important. The plasma protein binding adjusted animal data were then used with allometric scaling to predict human CL, t½ and $Vd_{SS.}$ Results were 7.6 mL/min/kg, 70.6 minutes and 0.87 L/kg, respectively. Based on the predicted human blood clearance and the dose required to image atherosclerosis in a rabbit model, the human dose would be unacceptably high. This demonstrates how allometric scaling can be used in research projects to assess clinical feasibility.

The impact of metabolic differences influencing the reliability of using different species to predict for man was highlighted by DPC-A78445-00. This agent is being developed as an alternative to exercise in myocardial perfusion imaging for the evaluation of coronary artery disease. DPC-A78445-00 was rapidly metabolized to the carboxylic acid by mouse and rat blood *in vitro* and *in vivo,* however, longer stability was observed in the dog. Human blood *in vitro* data were consistent with the dog data suggesting the mouse and rat would not be representative. DPC-A78445-00 plasma protein binding was at a similar, moderate level in rat, dog and human plasma, and metabolism by hepatocytes was rapid for all three species. Lave and co-workers, 1997, also found that using *in vitro* metabolism data (i.e. hepatocytes) to adjust allometric scaling dramatically improved the prediction of human clearance (80% to 40%) compared to the approach in which clearance is directly extrapolated using body weight. Phase I human clinical trial testing determined the area under the blood concentration-time curve (AUC) and clearance predicted by the dog were within 32% of the human values.

The research presented in this dissertation has identified that weight based allometric scaling of clearance from appropriate pre-clinical animal models can clearly be useful in predicting the human dose levels of imaging agents for Phase I clinical testing. It has also identified that allometric scaling of clearance from animal models when corrected for plasma protein binding yielded reliable predictions of the human clearance (differed by < 30%) for radiopharmaceutical imaging agents. Furthermore, the application of scaling models provided insight into the translation from pre-clinical

testing to human application and assessment of feasibility. The need to assess and select appropriate animal models that will represent the human was highlighted in the final chapter and emphasizes difficulty in trying to achieve models that will be robust and reliable across all situations.

Considering the following statements from colleagues in the field of pharmacokinetics, this research has proven consistent with their sentiments and extended the application of one approach into the radiopharmaceutical field.

"Although allometric scaling has much utility as a retrospective tool, like any other method its prospective applicability is not optimal" (Bonate *et al*, 2000). Nagilla and co-workers, 2005, believe that no single method identified to date offers the "perfect" solution, and welcomes ongoing efforts by the scientific community to continue to refine the peer-reviewed knowledge in this field.

6.1.2 Future Research

Future research in the area of predicting pharmacokinetics could include;

- Following the fate of the parent and metabolites over the entire blood concentration-time curve. This would provide a total “mass balance” of all forms of the drug within the blood circulation for determining full kinetic information related to protein binding, clearance rates and clearance routes of parent drug/metabolites.
- Investigating the accuracy of predicting toxicokinetics that are conducted with high doses of a test agent from pre-clinical studies typically done with low doses. Basically determining predictability through a range of doses and how saturating enzymes, receptors and clearance mechanisms may affect disposition of the drug.
- Determining a method to evaluate how to predict from animal models into a human with a known disease state. This may involve testing pre-clinical models with the disease or trying to model known variations caused by the human disease state and applying them to normal animal data.
- Investigating drug-drug interactions with respect to competing for protein binding, receptor binding or clearance mechanisms that may vary between species and affect predictive success.

These additional areas of investigation would provide significant information on the utility and capability of predicting human pharmacokinetics.

7. REFERENCES

Baker, R.J., D. Kozoll, and K.A. Meyer. 1957. The use of surface area as a basis for establishing normal blood volume. *Surg. Gynecol. Obstet.* 104:183-189.

Banavar, J.R., A. Maritan, and A. Rinaldo. 1999. Size and form in efficient transportation networks. *Nature* 399:130-132.

Barrett, J.A., M. Bresnick, A. Crocker, D.S. Edwards, S.J. Heminway, S. Liu, and T. Mazaika. Determination of the *in vitro* mechanism of action and *ex vivo* antiplatelet effects of XV066, a potential thrombus imaging agent.1995. DuPont Merck Radiopharmaceutical Discovery Research Report. RDR 95-01.

Benet, L.Z., N. Massoud, and J.G. Gambertoglio. Pharmacokinetic basis for drug treatment. Raven Press, New York, 1984.

Bentzon, J.F., G. Pasterkamp, and E. Falk. 2003. Expansive remodeling is a response of the plaque-related vessel wall in aortic roots of ApoE-deficient mice. *Arterioscler. Thromb. Vasc. Biol*. 23:257-262.

Bonate P.L., and D. Howard. 2000. Prospective allometric scaling: does the emperor have clothes?. *J Clin Pharmacol.* 40(4):335-340.

Bonati, M., R. Latini, and G. Tognoni. 1984. Interspecies comparison of *in vivo* caffeine pharmacokinetics in man, monkey, rabbit, rat, and mouse. *Drug Metab. Rev*. 15:1355-1383.

Boxenbaum, H. 1982. Interspecies scaling, allometry, physiological time, and the ground plan of pharmacokinetics. *J. Pharmacokin. Biopharm.* 10:201-227.

Brooks, P.C., R.A. Clark, and D.A. Cheresh. 1994. Requirement of vascular alpha v beta 3 from angiogenesis. *Science*. 5158:569-571.

Brooks, P.C., A.M. Montgomery, M. Rosenfeld, R.A. Reisfeld, and T. Hu, G. Klier, and D.A. Cheresh.1994. Integrin alpha v beta 3 antagonists promote tumor regression by inducing apoptosis of angiogenic blood vessels. *Cell.* 79(7):1157-1164.

Brooks, P.C. 1996. Role of integrin in angiogenesis. *Eur. J. Cancer*. 32A(14):2423-2429.

Buchwald, P. 2001. Structure-metabolism relationships: steric effects and the enzymatic hydrolysis of carboxylic esters. *Mini Rev. Med. Chem*. 1(1):101-111.

Calabrese, E.J. Principles of animal extrapolation. Lewis Publishers, Inc., Michigan, 1946 p. 107-108.

Calder, W.A. III. Size, function and life history. Harvard University Press, Massachusetts, 1984.

Caldwell, G.W., J.A. Masucci, Z. Yan, and W. Hageman. 2004. Allometric scaling of pharmacokinetic parameters in drug discovery: can human CL, Vd_{ss} and $t_{1/2}$ be predicted from in-vivo rat data? *Eur. J. Drug Metab. Pharmacokinet.* 29:133-143.

Cerqueira, M.D., M.S. Verani, M. Schwaiger, J. Heo, and A.S. Iskandrian. 1994. Safety profile of adenosine stress perfusion imaging: results from the adenoscan multicenter trial registry. *J. Am. Coll. Cardiol*. 23(2):384-389.

Crum-Brown, A. and T.R. Fraser. 1868-1869. *Trans. R. Soc. Edinburgh*. 25:151 and 693.

Davies, B., and T Morris. 1993. Physiological parameters in laboratory animals and humans. *Pharmaceutical Research*, 10(7):1093-1095.

Dedrick, R.L., K.B. Bischoff, and D.Z. Zaharko. 1970. Interspecies correlation of plasma concentration history of methotrexate (NSC-740). *Cancer Chemother. Rep. Part I.* 54:95-101.

DeNardo, S.J., G.L. DeNardo, A. Yuan, C.M. Richman, R.T. O'Donnell, P.N. Lara, D.L. Kukis, A. Natarajan, K.R. Lamborn, F. Jacobs, and C.L. Hartmann Siantar. 2003. Enhanced therapeutic index of radioimmunotherapy (RIT) in prostate cancer patients: comparison of radiation dosimetry for 1,4,7,10-tetraazacyclododecane-N,N',N'',N'''-tetraacetic acid (DOTA)-peptide versus 2IT-DOTA monoclonal antibody linkage for RIT. *Clin. Cancer Res.* 9:3938s-3944s.

Dodds, P.S., D.H. Rothman, and J.S. Weitz. 2001. Re-examiniation of the "3/4-law" of metabolism. *J. Theor. Biol*. 209:9-27.

Dreyer, G., and W. Ray. 1910. The blood volume of mammals as determined by experiments upon rabbits, guinea pigs and mice and its relationship to the body weight and to the surface area expressed as a formula. *Philos. Trans. R. Soc. London Ser. B.* 201:133-160.

Feldman, H.A. and T.A. McMahon. 1983. The ¾ mass exponent for energy metabolism is not a statistical artifact. *Respir. Physiol*. 52:149-163.

Feldman, L.J., M. Mazighi, A. Scheuble, J.F. Deux, E. De Benedetti, C. Badier-Commander, E. Brambilla, D. Henin, P.G. Steg, and M.P. Jacob. 2001. Differential expression of matrix metalloproteinases after stent implantation and balloon angioplasty in the hypercholesterolemic rabbit. *Circulation*. 103:3117-3122.

Focan, C., M.P. Graas, M. Beauduin, J.L. Canon, J.P. Salmon, G. Jerusalem, D. Focan-Henrard, J.P. Lobelle, and D. Schallier. 2005. Sequential administration of epirubicin and paclitaxel for advanced breast cancer. A phase I randomised trial. *Anticaner Res*. 25(2B):1211-1217.

Glover, D.K., M. Ruiz, K. Takehana, F.D. Petruzella, L.M. Riou, J.M. Rieger, T.L. Macdonald, D.D. Watson, J. Linden, and G.A. Beller. 2001. Pharmacological stress myocardial perfusion imaging with the potent and selective A(2A) adenosine receptor agonists ATL193 and ATL146e administered by either intravenous infusion or bolus injection. *Circulation*. 104(10):1181-1187.

Goldstein, A. 1949. The interactions of drugs and plasma proteins. *Pharmacol. Rev.* 1:102-165.

Gorman, C., D. Onthank, N. Williams, S. Robinson, and D.S. Edwards. 2003. Development of a high sensitivity LC/MS/MS method for the quantitation of DPC-A78445, a novel pharmacological stress agent in rodent, canine and human blood. American Society of Mass Spectrometry annual meeting poster session. Toronto, Canada.

Hendel R.C., T. Jamil, and D.K. Glover. 2003. Pharmacologic stress testing: New methods and agents. J. *Nucl. Cardiol.* 10:197-204.

Heusner, A.A. 1982. Energy metabolism and body size. I. Is the 0.75 mass exponent of Kleiber's equation a statistical artifact? *Respir. Physiol*. 48:1-12.

Johnson, J.L., and C.L. Jackson. 2001. Atherosclerotic plaque rupture in the apolipoprotein E knockout mouse. *Atherosclerosis*. 154:399-406.

Johnstone, M.T., R.M. Botnar, A.S. Perez, R. Stewart, W.C. Quist, J.A. Hamilton, and W.J. Manning. 2001. *In vivo* magnetic resonance imaging of experimental thrombosis in a rabbit model. *Arterioscler. Thromb. Vasc. Biol*. 21:1556-1560.

Kleiber, M. 1932. Body size and metabolism. *Hilgardia* 6:315-353.

Koch-Weser, J. and E.M. Sellers. 1976. Binding of drugs to serum albumin. Parts I and II. *N. Eng. J. Med*. 294(6):311-316; 294(10):526-531.

Kwiatkowski, R. Canadian handbook on health impact assessment: volume 3: roles for the health practitioner. 1999.

Lave, T., S. Dupin, C. Schmitt, R.C. Chou, D. Jaeck, and P. Coassolo. 1997. Integration of *in vitro* data into allometric scaling to predict hepatic metabolic clearance in man: Application to 10 extensively metabolized drugs. *J. Pharm. Sci.* 86(5):584-586.

Lombardo, F., R.S. Obach, M.Y. Shalaeva, and F. Gao. 2002. Prediction of volume of distribution values in humans for neutral and basic drugs using physicochemical measurements and plasma protein binding data. *J. Med. Chem*. 45:2867-2876.

Mahmood, I. And J. D. Balian. 1996. Interspecies Scaling: A comparative study for the prediction of clearance and volume using two or more than two species. *Life Sciences.* 59(7):579-585.

Mahmood, I. 1998. Allometric issues in drug development. *J. Pharm. Sci.* 88(11):1101-1106.

Meyer, M.C., and D.E. Guttman. 1968. The binding by plasma proteins. *J. Pharm. Sci.* 57:895-918.

Minagawa, T., Y. Kohno, T. Suwa, and A. Tsuji. 1995. Species differences in hydrolysis of isocarbacyclin methyl ester (TEI-9090) by blood esterases. *Biochemical Pharmacology*. 49(10):1361-1365.

Mordenti, J. 1985. Pharmacokinetic scale-up: accurate prediction of human pharmacokinetic profiles from animal data. *J. Pharm. Sci.* 74(10):1097-1099.

Mordenti, J. 1986. Man vs. beast: pharmacokinetic scaling in mammals. *J. Pharm. Sci.* 75:1028-1040.

Nagilla, R., and K.W. Ward. 2004. A comprehensive analysis of the role of correction factors in the allometric predictivity of clearance from rat, dog, and monkey to humans. *J. Pharm. Sci*. 93:2522-2534.

Nagilla, R. and K.W. Ward. 2005. The correction factors do help in improving the prediction of human clearance from animal data. Reply to comments. *J. Pharm. Sci*. 94(5):946-947.

Onthank D.C., S. Liu, P.J. Silva, J.A. Barrett, T.D. Harris, S.P. Robinson, and D.S. Edwards. 2004. ^{90}Y and ^{111}In complexes of a DOTA-conjugated integrin $\alpha_v\beta_3$ receptor antagonist: different but biologically equivalent. *Bioconjugate Chem.* 15:235-241.

Pinkel, D. 1958. The use of body surface area as a criterion of drug dosage in cancer chemotherapy. *Cancer Res.* 18:853-856.

Plow E.F., G. Marguerie,and M. Ginsberg. 1987. Fibrinogen, fibrinogen receptors and the peptides that inhibit these interactions. *Biochem Pharmacol*. 36:4035-4041.

Ranhosky, A., J. Kempthorne-Rawson. 1990. The safety of intravenous dipyridamole thallium myocardial perfusion imaging. Intravenous dipyridamole thallium imaging study group. *Circulation*. 81(4):1205-1209.

Rosenfeld, M.E., P. Polinsky, R. Virmani, K. Kauser, G. Rubanyi, and S.M. Schwartz. 2000. Advanced atherosclerotic lesions in the innominate artery of the ApoE knockout mouse. *Arterioscler. Thromb. Vasc. Biol.* 20:2587-2592.

Sakata, C., H. Tanaka, S. Takemura, Y. Minamiyama, A. Nakamura, K. Katsuragi, H. Huang, S. Kubo, K. Hirohashi, and H. Kinoshita.1999. Effect of intraportal infusion of adenosine on hepatic blood flow and injury after ischemia and reperfusion of canine liver. *Transplantation Proceedings.* 31:509-510.

Satoh, T., and M. Hosokawa. 1998. The mammalian carboxylesterases: from molecules to functions. *Annu. Rev. Pharmacol. Toxicol*. 38:257-288.

Schmidt-Nielsen, K. Scaling: Why is animal size so important? Cambridge University Press, New Jersey, 1983.

Silverman, R.B.The organic chemistry of drug design and drug action. Academic Press, Inc., New York, 1992 p11-15.

Sosnovik, D.E., J.E. Muller, S. Kathiresan, and T.J. Brady. 2002. Non-invasive imaging of plaque vulnerability: and important tool for the assessment of agents to stabilize atherosclerotic plaques. *Expert Opin. Investig. Drugs.* 11(5):693-704.

Tager A.M., and A.D. Luster. 2003. BLT1 and BLT2: the leukotriene B(4) receptors. *Prostaglandins Leukot Essent Fatty Acids*. 69(2-3): 123-134.

Tang, H., and M. Mayersohn. 2005. A novel model for prediction of human drug clearance by allometric scaling. *Drug Metab. Disp.* 33:1297-1303.

Tang, H., and M. Mayersohn. 2005. Accuracy of allometrically predicted pharmacokinetic parameters in humans: role of species selection. *Drug Metab. Disp.* 33:1288-1293.

Van Eerd, J.E., W.J. Oyen, T.D. Harris, H.J. Rennen, D.S. Edwards, S. Liu, C.E Ellars, F.H. Corstens, and O.C. Boerman. 2003. A bivalent leukotriene B(4) antagonist for scintigraphic imaging of infectios foci. *J. Nucl. Med.* 44(7):1087-1091.

Varner, J.A., P.C. Brooks, and D.A. Cheresh. 1995. Review: the integrin alpha v beta 3: angiogenesis and apoptosis. *Cell Adhes. Commun*. 3(4):367-374.

Weiss, M., W. Sziegoleit, and W. Forster. 1977. Dependence of pharmacokinetic parameters on the body weight. *Int. J. Clin. Pharmacol. Ther. Toxicol.* 15:572-575.

West, G.B., J.H. Brown, and B.J. Enquist. 1997. A general model for the origin of allometric scaling laws in biology. *Science*. 276:122-126.

West, G.B., J.H. Brown, and B.J. Enquist. 1999. The fourth dimension of life: fractal geometry and allometric scaling of organisms. *Science.* 284:1677-1679.

Williams, R.T. 1967. Comparative patterns of drug metabolism. *Fed. Proc*. 26(4):1029-1039.

Witiak, D.T., and M.W. Whitehouse. 1969. Species differences in the albumin binding of 2,4,6-trinitrobenzaldehyde benzoic acid and some other acidic drugs – The unique behavior of rat plasma albumin. *Biochem. Pharmacol*. 18:971-977.

8. APPENDIX

8.1 **Onthank D.C., S. Liu, P.J. Silva, J.A. Barrett, T.D. Harris, S.P. Robinson, and D.S. Edwards. 2004. ^{90}Y and ^{111}In complexes of a DOTA-conjugated integrin $\alpha_v\beta_3$ receptor antagonist: different but biologically equivalent. *Bioconjugate Chem.* 15:235-241.**

(Attached as PDF file)